REPORT

U.S. DEPARTMENT OF TRANSPORTATION – PIPELINE AND HAZARDOUS MATERIALS SAFETY ADMINISTRATION

INTERNAL CORROSION DIRECT ASSESSMENT DETECTION OF WATER (WP #205)

REPORT NO EAWUS811-80612405

REVISION NO 2

DET NORSKE VERITAS

INTERNAL CORROSION DIRECT ASSESSMENT DETECTION OF WATER (WP #205)

Client:
U.S. DEPARTMENT OF TRANSPORTATION – PIPELINE AND HAZARDOUS MATERIALS SAFETY ADMINISTRATION

DNV COLUMBUS

5777 Frantz Road
Dublin, Ohio 43017-1386
U.S.A.
Tel: (614)761-1214
Fax: (614)761-1633
http://www.dnvcolumbus.com

Report No.: EAWUS811-80612405 Subject Group:

Indexing terms:

Summary:

Prepared by: *C. Sean Brossia*
Head of Section – Technology Development
Signature

Verified by: *Oliver Moghissi*
Head of Department – Corrosion and Materials Technology Center
Signature

Approved by: *Oliver Moghissi*
Head of Department – Corrosion and Materials Technology Center
Signature

Date of issue: 12/31/2008

Project No: 80612405

- [x] No distribution without permission from the client or responsible organizational unit (however, free distribution for internal use within DNV after 3 years)
- [ ] No distribution without permission from the client or responsible organizational unit
- [ ] Strictly confidential
- [ ] Unrestricted distribution

All copyrights reserved DNV Columbus. This publication or parts thereof may not be reproduced or transmitted in any form or by any means, including photocopying or recording, without the prior written consent of DNV Columbus.

DRAFT FINAL REPORT

Table of Contents *Page*

1 INTRODUCTION AND BACKGROUND 2

2 APPROACH 4
2.1 Overall Conceptual Designs 5

3 RESULTS AND DISCUSSION 7
3.1 Corrosivity Sensor Optimization 7
3.1.1 Sensor Life 8
3.1.2 Sensor Sensitivity 9
3.2 Sensor Packaging 12
3.2.1 Sensor Durability 13
3.2.2 Solid Spherical Packaging 16
3.2.3 Hollow Package Designs 17
3.2.3.1 Off the Shelf Hollow Spheres 18
3.2.3.2 Cast Epoxy Shell Spheres 19
3.2.3.3 Spheres with Recessed Shells 20
3.2.4 Creep Testing of Nested Sphere Packaging Scheme 21
3.3 Sensor Design, Location and Communications 23
3.3.1 Sensor Location Tracking 28
3.3.1.1 Time Domain Reflectometry 28
3.3.1.2 Acoustic Ranging 29
3.3.1.3 Optical Translation Measurement 29
3.3.1.4 Ultra Wideband Ranging 29
3.3.1.5 WiFi Mote Ranging 33
3.4 Sensor Injection and Retrieval Systems 35
3.5 Flow Loop Validation Trials 36
3.5.1 Initial Low Pressure Loop Tests 36
3.5.2 High Pressure Flow Loop Tests 44
3.5.3 Flow Loop Sensor Validation Trials 46

4 CONCLUSIONS AND TECHNOLOGY IMPLEMENTATION 51

Reference to part of this report which may lead to misinterpretation is not permissible.

1 INTRODUCTION AND BACKGROUND

Internal corrosion of natural gas pipelines is the result of interaction between the inside pipe wall and impurities in the product being transported. Such interactions can lead to an overall loss of material thereby thinning the pipe wall and thus reducing the range of operating pressure. Corosion, however, tends to be localized along the pipeline with some areas experiencing significant corrosion rates and others much less so. Part of the variability arises from both spatial and temporal differences in the composition of the product. For example, brines may be observed in segments of natural gas pipelines close to producing areas (i.e., carry-over produced water), but condensed water are more likely further downstream (i.e., without chlorides). Some of the common corrosion inducing species includes carbon dioxide, hydrogen sulfide, water, salts (such as chloride), solids and precipitates, organic acids, and microorganisms. As a consequence of the wide range of possible corrosion inducing species, their inherent variability with both position and time within the pipeline, accurate inspection and determination of the true condition within the pipeline is difficult.

Over the last several years, The Office of Pipeline Safety attributes approximately 14 and 12% of natural gas and liquids transmission pipelines accidents, respectively, to internal corrosion. These incidents include some high profile failures involving fatalities, service/deliverability interruption, and environmental damage. Public safety concerns have provided the driving force for new regulations that require pipeline integrity assessments. There are currently three available pipeline assessment methodologies: (a) in-line inspection (ILI), (b) hydrostatic testing, and (c) direct assessment. Depending on the pipeline conditions the appropriate methodology can be used.

In-line inspection (ILI) is capable of detecting internal corrosion. The ability of this technique to find corrosion flaws larger than a certain size (10 percent of pipe wall thickness) makes it extremely valuable for locating flaws before they become critical and cause pipeline failure (either leaks or rupture)). ILI methods include ultrasonic transmission and magnetic flux leakage. In these cases, the necessary instrumentation is mounted on a tool (pig) that travels inside the pipeline. ILI tools are 3.0 to 5.5 m (10 to 18 ft) in length. The ILI tools must be capable of readily passing through the pipeline and the sensors must be able to produce good contact (MFL tool) or stand-off from the pipe wall (UT tool). For these reasons, pipelines with large buckles, large dents, tight-radius bends, or valves that do not open fully can provide difficulty in conducting an inspection and, in some cases, will cause limitations that make the lines not “piggable”. The tool will simply not fit through the pipeline. In addition, pipelines to be inspected by ILI tools must be fitted with launchers and retrievers. Nearly 30% of the natural gas pipelines in the United States are not piggable.

Another well known inspection technique is hydrostatic testing. This however requires a service interruption and has technical drawbacks as an assessment method (e.g., detecting leak without rupture). Another common method for inspection of internal corrosion is insertion of

coupons into the pipeline. The main limitation with coupons is that they cannot always be placed at locations that are most likely to experience corrosion. In addition, they only provide a time-averaged indication of the rate of corrosion. That is, the corrosion that is noted on the coupon is assumed to have occurred over the entire time the coupon is in place, when in reality the corrosion may have occurred only during a very short duration giving rise to a significant underestimation of the corrosion rate.

Internal Corrosion direct Assessment (ICDA) was developed for gas transmission lines that normally carry dry gas but may suffer from short term upsets of liquid water. The ICDA methodology for dry gas relies on established multiphase flow principles to predict locations of water accumulation. For the nominally dry gas lines, a simple correlation was developed that calculates the critical angle of inclination for water accumulation that can be compared to the actual angle of inclination of the pipe (measured by digital elevation data and depth of cover). Once critical angle sites are identified, the pipe is excavated and one or more direct examination techniques (e.g., ultrasonic inspection) are used to determine whether internal corrosion is present. Depending on these direct examinations, further inspections may be necessary. A previous study by one of the investigators in a project funded by DOT (Contract No. DTRS5603T0001, Internal Corrosion Direct Assessment of Gas Transmission and Storage Lines) identified several issues:

- The uncertainties in flow modeling parameters and pipeline inclination angles resulted in considerable uncertainty in the location of water hold-up.
- The ICDA procedure does not provide information on the length of pipe to excavate. This could be a significant problem for long slopes as shown in Figure 1.
- After ICDA, obtaining the necessary access to sites for pipe excavation can often be prohibitively expensive.
- Even if locations of water accumulation are identified, the extent of corrosion or the corrosivity of the water is unknown.
- Non-intrusive monitoring devices, such as the Field Signature Method (FSM), are point monitors. Estimation of corrosivity at a number of locations may assist in confirmatory direct assessment and estimating the reassessment interval.

Because of the uncertainties related to ICDA and constraints making some pipelines un-piggable in the traditional sense, other technologies and alternative methods for pipeline inspection have been examined. In the present work, recent advances in computer technologies and wireless communications have been leveraged and combined in an attempt to address some of the challenges faced by the internal corrosion pipeline community.

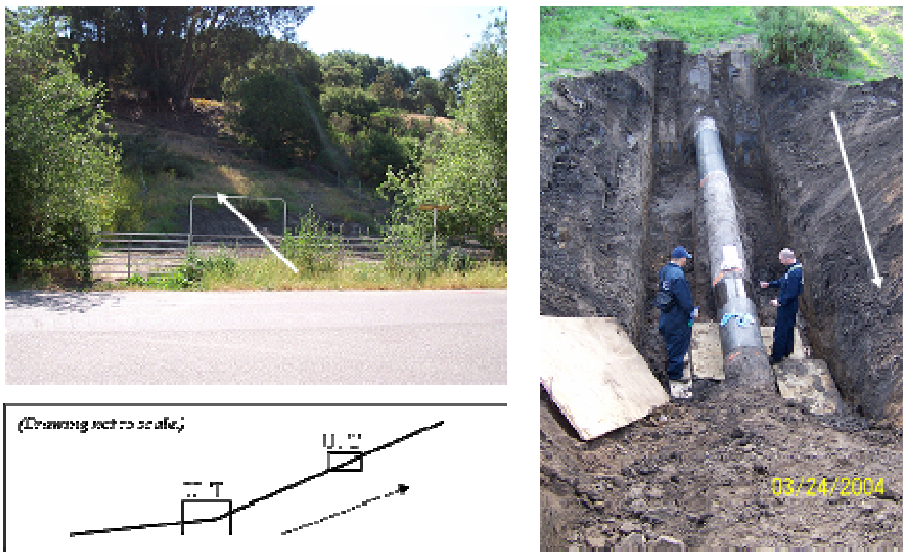

Figure 1. Uncertainty in the extent of pipe to be excavated for ICDA

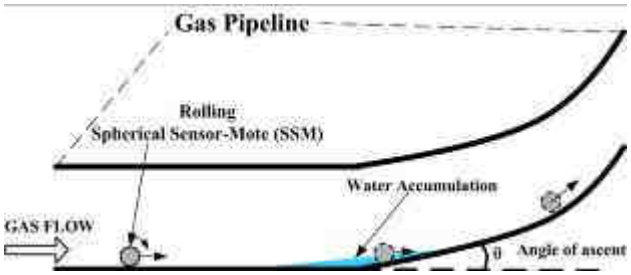

Figure 2. Illustration showing fluidized sensor motion

2 APPROACH

The overall approach was to develop and evaluate a sensor platform that could detect water accumulation, provide its approximate location along the pipeline, and estimate the corrosivity of any liquids found. To accomplish this, a spherical sensor system has been developed and evaluated that consists primarily of a microprocessor with wireless

communications capability and a corrosivity or corrosion rate sensor and is in the form of a small sphere (~1.5” diameter) that behaves fluid dynamically similar to entrained water in a gas stream (schematic shown in Figure 3). Previous testing confirmed that wireless communications between two microprocessor units (called Motes) inside a pipeline was not only feasible but actually showed enhancement compared to communication in air resulting from the inner pipe wall acting as a wave guide.

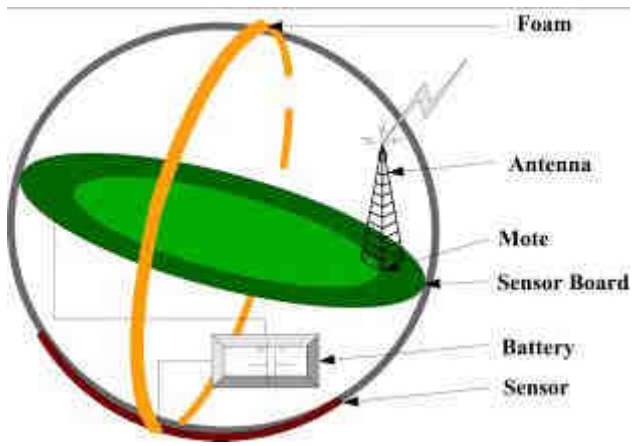

Figure 3: Illustration of spherical sensor.

Suitable corrosivity/corrosion rate sensors have also been developed that show excellent environmental selectivity (i.e., the sensor can distinguish between a highly corrosive environment and a relatively benign environment) as well as superior correlation to corrosion rate. Lastly, computational fluid dynamics modeling confirmed that the spherical sensor motes (SSM) indeed can behave similar to entrained water and can collect at locations where water accumulation is predicted by the ICDA methodology.

2.1 Overall Conceptual Designs

During the course of the project, two operational conceptual design alternatives emerged based on pipeline operator inputs. The first, which was the original intent of the project, was to create a “leave in place” sensor system. In this, configuration multiple sensors will be injected into a transmission pipeline to monitor for water accumulation at a specific location of interest (e.g., road crossing, critical incline, etc.). A schematic diagram of this configuration is shown in Figure 4. As part of the internal corrosion monitoring scheme, the sensors will be injected upstream of the location of interest (preferably within 300-1000’; likely closer). It is anticipated that up to 6 – 12 sensors or more could be injected and allowed to flow from in the injection point to the location of interest. Once on station, the sensors will be left in place for a period of

up to perhaps several years. The nominal life expectancy of the power cell (battery) used should provide approximately 200-300 measurements. Thus, depending on the frequency at which the measurements are taken, the life expectancy of the sensors could be considerable (e.g., if only one measurement per week is taken, an operational life of between 4 – 6 years is expected). An alternative would be to introduce a series of sensors with different data acquisition rates (and thus different life expectancies). Regardless of the initial configurations and choices made, because additional sensors can be introduced some flexibility exists. Once the sensors are no longer functional, the plan would be to use a cleaning pig to sweep them out.

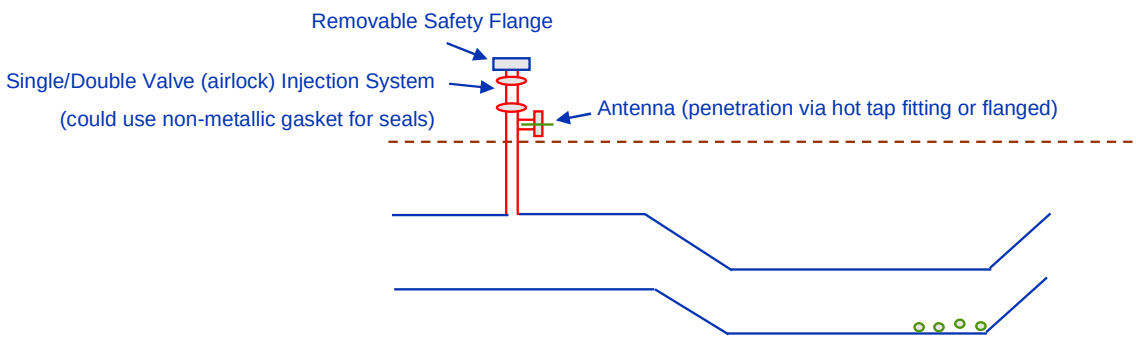

Figure 4: Schematic of "leave in place" configuration.

The second configuration design concept that was envisioned is a “once-through” type system. In this configuration, a mobile version of the sensor system would be used. These sensors will be injected upstream of a location of interest and will flow to a suitable location downstream. Between the injection and retrieval points, the sensors will be continually flowing, collecting data, and storing the data in memory which will be accessed after completing the run. A schematic diagram of this arrangement wherein the sensors are collected at a drip is shown in Figure 5.

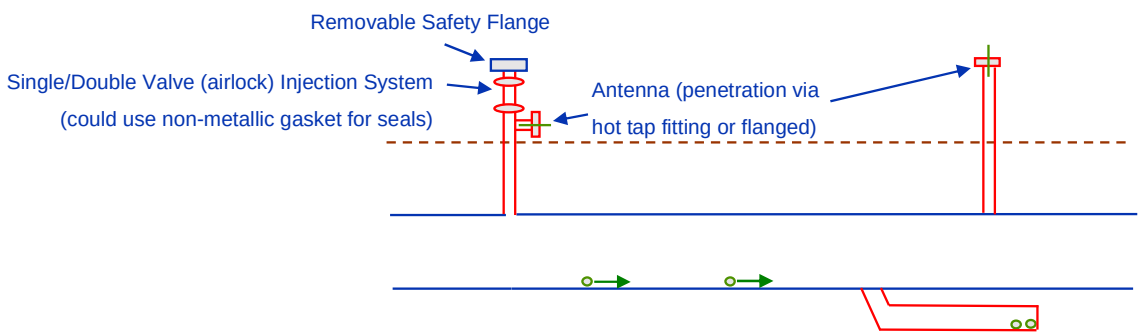

Figure 5: Schematic diagram of flow through field validation test on gathering line using a drip to collect the sensors.

From a configuration and components standpoint, both sensor designs would be comprised of the same microprocessor, wireless communications, and corrosivity sensors. The main differences between the units would be the power systems (battery) and perhaps memory capacity. Both unit types would be batter powered but because of the desired long life for the leave in place variation, a higher energy density may be advisable. Though both unit types would have flash memory, the once through type would require more memory capacity since all measurements during the "inspection" run would be stored on board for later download rather than the periodic download planned for the leave in place version.

3 RESULTS AND DISCUSSION

Over the course of the project, efforts were aimed at five principal activities:

- Optimization of the corrosivity sensor: though the thin film corrosivity sensors utilized in this project were essentially commercial off the shelf technologies, some optimization and modifications to better suit pipeline operating conditions were needed
- Packaging the sensor: to enable wireless communications, the sensor package could not be constructed from a metallic sphere; thus an examination and design of polymeric spheres that could withstand pressures > 1,000 psi was needed
- Providing sensor location and communications: several different sensor location and communication technologies were examined during the project; some technologies at first appeared viable but further evaluation proved that they were not acceptable; in other cases, advances in communications technology, independent of this project, resulted in various alternatives being explored
- Evaluating possible sensor injection and retrieval systems: getting the sensors into and out of the pipeline is critically important and some simple methods to accomplish this were examined
- Flow loop validation trials: after each of the individual systems and components (e.g., packaging shell, wireless communications, corrosivity sensor, etc.) were evaluated and validated, fully functioning prototype sensors were constructed and then tested in flow loop tests

Each of these activities is discussed below.

3.1 Corrosivity Sensor Optimization

Modification of the interdigitated sensors to be used in fluidized sensor packages for direct assessment of internal corrosion of gas transmission pipelines focused on sensor electrode

composition, and sensor pattern. The sensor pattern was studied previously, and found to be an insignificant parameter in fabrication of these sensors. This suggests that the sensor itself may be patterned to fit the specific application, as long as the fundamental components are maintained (i.e., sensor concept and measurement technique). Therefore, recent efforts were focused on optimizing the composition of the corrosion sensitive electrode. This optimization would follow two design criteria:

1. improve resilience to corrosive attack in an H2S/CO2 pipeline environment, and
2. maintain a high sensitivity to detecting corrosivity.

To achieve this, it was hypothesized that adding controlled amounts of Cr to the Fe (sensitive) electrode would improve the resilience of the sensor, while maintaining an adequate level of sensitivity towards detecting corrosivity of a liquid towards carbon steel as long as Cr-levels did not exceed 12-13%, the level required to make steel 'stainless'. Cr could be added to Fe in the sputtering process rather easily, so the sensor modification would not be costly or time consuming. Since the original geometry of the interdigitated electrode was maintained, generated data could be directly compared to the original data to see whether improved sensor performance was achieved.

3.1.1 Sensor Life

Initial evaluation of the Fe-Cu interdigitated sensor included exposing this sensor to an H_2S/CO_2 containing environment that simulated the conditions inside a pipeline. The purpose of this testing was to determine how the metallic sensor elements of the sensor would survive in this potentially corrosive environment. If the sensor elements did show significant levels of corrosion, their ability to record a representative corrosivity measurement would be diminished and the sensor rendered useless.

To simulate a pipeline environment, a stainless steel autoclave was partially filled with deionized water, and pressurized to 500 psi with a gas mixture of 1% CO_2 - 0.01% H_2S - bal N_2, a mixture that contains CO_2 and H_2S in their likely concentrations for piped natural gas. Under pressure, these gases are expected to dissolve in the water, and turn the aqueous solution acidic. The acid solution may then corrode the metal components of the sensor, depending upon their vulnerability.

For sensors containing a pure Cu, and a pure Fe electrode, exposure to the simulated environment completely destroyed the metallic elements. Therefore, evaluation of Cr-containing elements would be obtained through visual inspection of the sensors after exposure to this environment for controlled lengths of time. Images of one week exposed sensors at each of the tested concentrations are shown below (Figure 6).

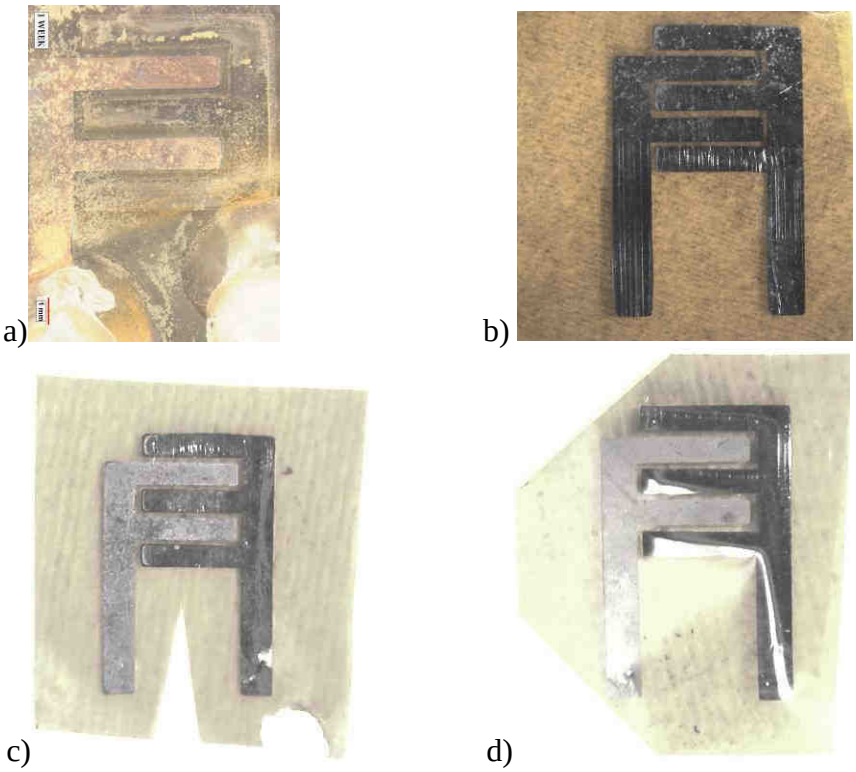

Figure 6: Images of (a) pure Fe, (b) 10 at% Cr/Fe, (c) 12 at% Cr/Fe, and (d) 16 at% Cr/Fe sensors after 1 week of exposure to simulated pipeline conditions.

The pure Fe electrode (a) was completely destroyed within a week of exposure, while all of the Cr containing sensors remained intact when subjected to the H_2S/CO_2 environment. From these findings it is apparent that adding Cr to the Fe electrode for the levels studied makes the sensor element more resilient to attack in the acidic environment. Visual inspection yielded no significant discrepancies between the varying levels of Cr, as none of these elements showed any signs of attack. Therefore it was concluded that adding Cr to the sensor elements in the concentrations tested made the sensors immune to chemical attack in the pipeline environment.

In addition, sensors a, c and d all have Cu secondary electrodes which were severely corroded by the simulated environment, while b did not. The effect of a corroded Cu element on the accuracy of the sensor measurement has not been tested. Since the Fe/Cr electrodes can withstand the environment, it was decided to make both sensor electrodes Fe/Cr (as in sensor b) and thereby avoid any possible, deleterious effects of a corroded Cu element. The second electrode is less crucial than the Cu, and no obvious side-effects of switching its composition to Fe/Cr was noted when making measurements with this sensor.

3.1.2 Sensor Sensitivity

While adding Cr makes these elements more resilient to attack, it may also deaden their sensitivity to corrosivity. The Fe electrode is the sensitive electrode of the original two electrode design, and changing its chemical composition may alter its sensitivity to detecting corrosive conditions. Therefore, Cr-containing sensors were immersed in a series of liquids having varying corrosivity towards carbon steel, but similar conductivity as was done for the original pure Fe sensor. The liquids consisted of 0.1 M NaCl, 0.1M NaCl and 0.1M $NaHCO_3$, and 0.1M $NaHCO_3$. These solutions were tested as they have similar conductivities, but NaCl is corrosive towards carbon steel while $NaHCO_3$ is passive. Since the sensor measurement involves making a resistance measurement, these liquids are an ideal test as they verify that the sensor measurement is indicative of corrosivity rather than conductivity, as the two are not always interchangeable. The sensors were tested by immersing in the solutions for one minute, and recording the sensor reading at 10 second intervals. The time dependent reading also gives insight into how quickly the sensors will yield a representative measurement, an important design consideration for a fluidized sensor package. The results for these tests are shown below in Figure 7.

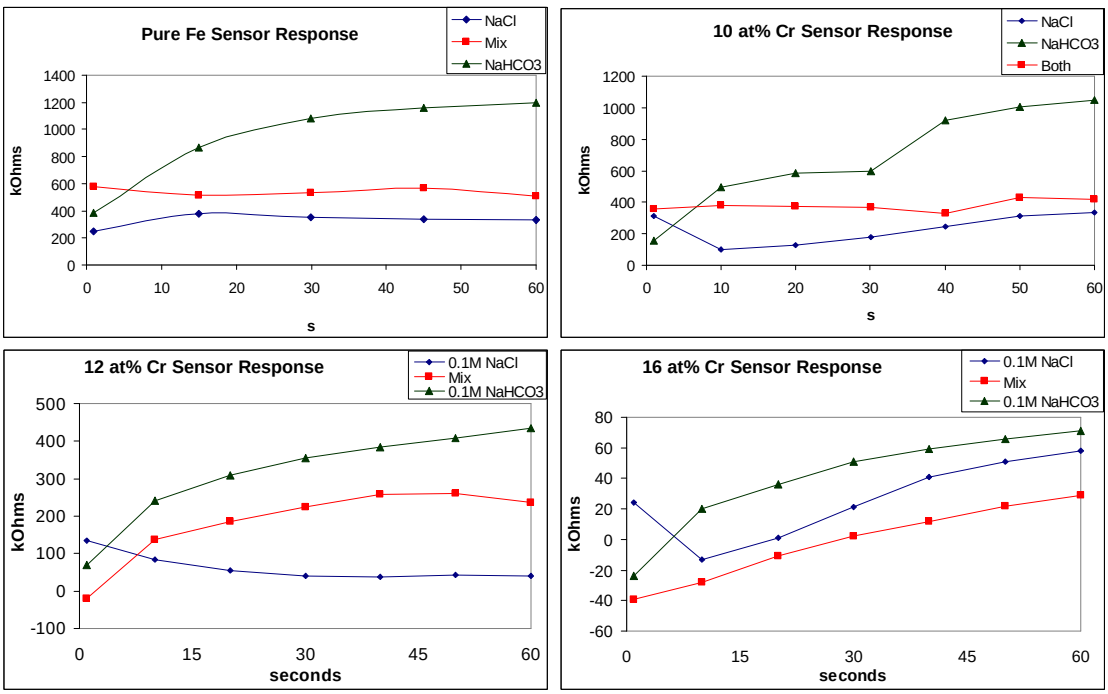

Figure 7: Measurement response to test solutions for interdigitated sensors of varying Cr concentrations.

To better illustrate the sensitivity of the sensors as a function of chromium concentration, Figure 8 shows the difference in recorded measurements between the NaCl and $NaHCO_3$ solutions after immersion for 60 seconds of immersion.

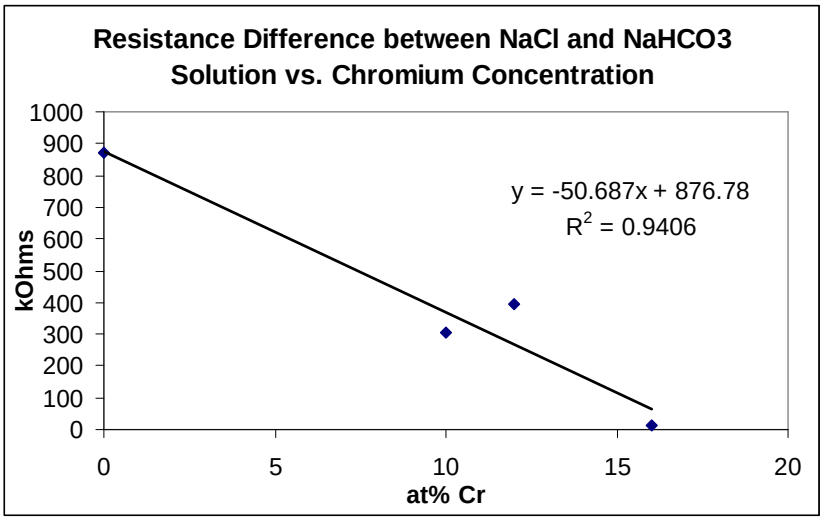

Figure 8: Sensitivity of sensors as a function of the chromium concentration of the sensor element.

Figure 8 shows that the sensitivity of the sensors decreases as the Cr concentrations increase, and seemingly, for every 1% increase in Cr, the difference in magnitude between the solutions (sensitivity) decreases by about 50 kOhms, as long as the sensor response is allowed to stabilize for 60 seconds. For measurement times shorter than 60 s, Figure 9 illustrates the time-dependent measurement sensitivity.

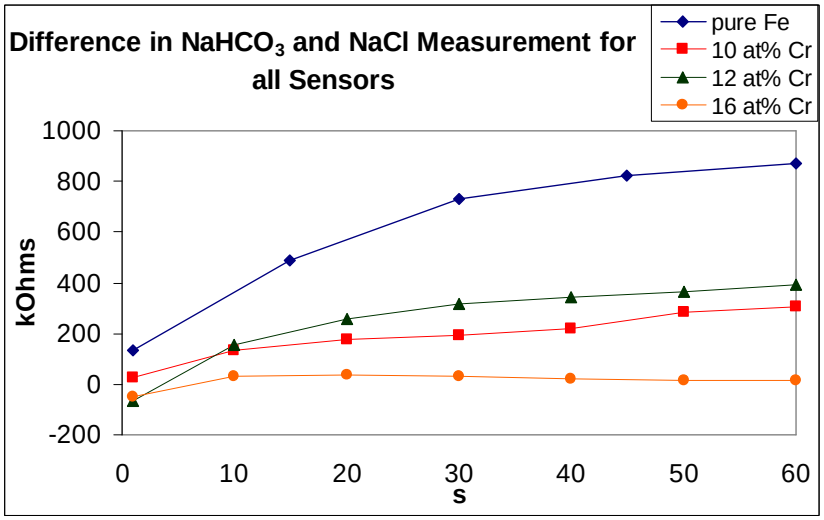

Figure 9: Time dependent sensitivity of all sensors tested.

All sensors showed increasing sensitivity with measurement time, although the overall sensitivity was still governed by Cr content (Figure 8). The time required to obtain sensitive-enough measurements to discern corrosivity depends upon the detection limits of the controlling electronics, which have yet to be verified. For the suggested sensor electronics specifications

submitted to Aginova Inc., sufficient sensitivity would be achieved within 10 seconds, while mere detection of liquid (evident by a non-zero sensor reading) may be obtained in the mere fraction of a second that the electronics require to execute a reading.

Sensitivity is shown to be inversely proportional to the resilience of the sensors in the H_2S/CO_2 exposure studies, as expected. There exists a trade-off with these sensors between resilience and sensitivity when adding Cr. The more sensitive the sensor to detect corrosion, the more likely it will be consumed when making the measurement. Conversely, the more robust the sensor in regards to resisting chemical attack, the less sensitive it is to discerning corrosivity of liquids in contact with the sensor. Although, no significant differences in visual appearance were noted for H_2S/CO_2 exposed Cr-containing sensors, all seemed unaffected by the exposure to the pipeline environment. An ideal sensor would have enough resilience in the pipe environment to maintain the integrity of its sensor electrode, while providing the maximum level of sensitivity to corrosivity. The latter ability may depend on the detection limits of the controlling electronics, especially when noting that the magnitude of resistance also has a dependence upon the Cr concentration (Figure 10). As neither the resident time in the pipeline environment, nor the detection limits of the controlling electronics been determined, the Cr concentrations may need to be adapted to the future constraints imposed by these variables as they become known.

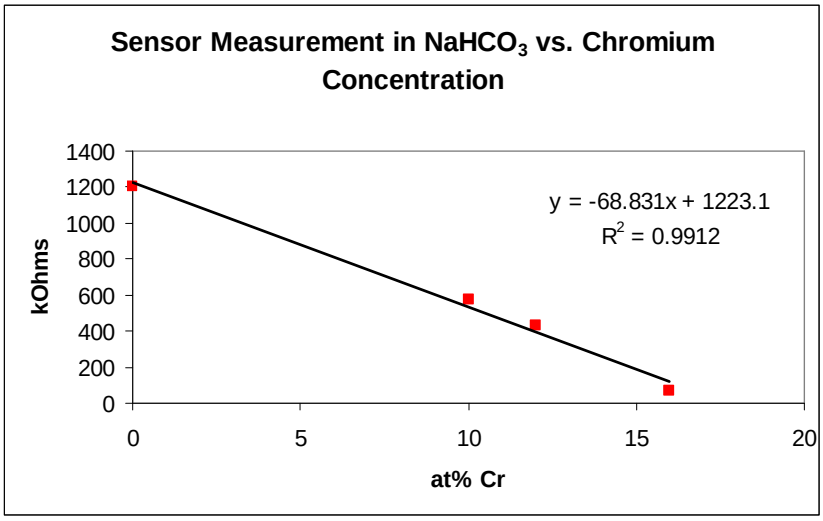

Figure 10: Measurement dependence upon chromium concentration of the sensor element.

3.2 Sensor Packaging

The sensor packaging design followed these guidelines:

1) protect the electronics as they propagate through the pipeline,
2) be of spherical shape for efficient flow,
3) have a mass of ~20 grams to meet the mass requirements for fluid flow calculations,
4) be transparent to E-M communication,
5) survive the pipeline environment for typical run duration of 4 hours.
6) be cost effective for a disposable product.

Two main activities were examined in this area including corrosivity sensor durability (as it related to overall sensor packaging) and the packaging itself either as a solid epoxy ball or as a hollow sphere.

3.2.1 Sensor Durability

The durability of the thin-film corrosivity sensor as the "skin" of the fluidized sensor package is an important design consideration for development of the sensor, as the sensor needs to reliably contact any liquids encountered in the pipe. The coupling of the sensor to the fluidized package could encompass many configurations, with perhaps the simplest being to adhere a Kapton®-backed sensor to the ball's outer surface. This method would allow for easy replacement of used sensors without intrusion into the electronics enclosure or structure of the package. This design, however, may give rise to complications in ensuring the integrity of the sensor as it is subjected to wear against the pipe wall during propagation down the pipeline. To better understand the wear and tear on the sensor with this design, a durability test was performed.

To simulate a sensor package, thin film sensors were adhered to the skin of a 2 in diameter polymer sphere with "5-minute" epoxy. 3 sensors in total were placed on the ball at orthogonal positions to each other (see Figure 11).

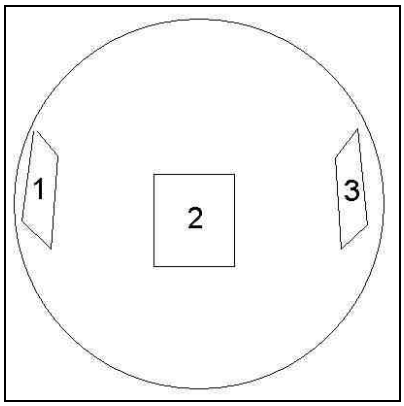

Figure 11: Location of sensors on ball for durability test.

Strips of duct tape sealed the perimeter of the adhered sensors to prevent peeling of the sensor during testing . The ball was then injected with water to yield a sensor package mass of 61.5g. This is over twice the planned weight of the fluidized sensor package, but was used to exaggerate any signs of wear on the sensor surface. The sensor package was then placed in a RO-TAP Testing Sieve Shaker for ten minutes. This machine is similar to a "paint shaker" and mechanically perturbs an attached compartment in a looping manner. The compartment consisted of an 8-in. diameter section of aluminum pipe having 3/8" wall thickness. The RO-TAP operates at 150 RPM, and the motion of the chamber was assumed to rotate the ball around the lower diameter of the cylinder at the same rate. A simple calculation based on the assumed motion indicates that a ten minute test would simulate the ball rolling down a 3150' length of pipe. After completion of the test the sensors were visually examined for evidence of wear. Images of the tested sensors are shown in Figure 12. Areas where the sensor electrode has been completely worn away are circled.

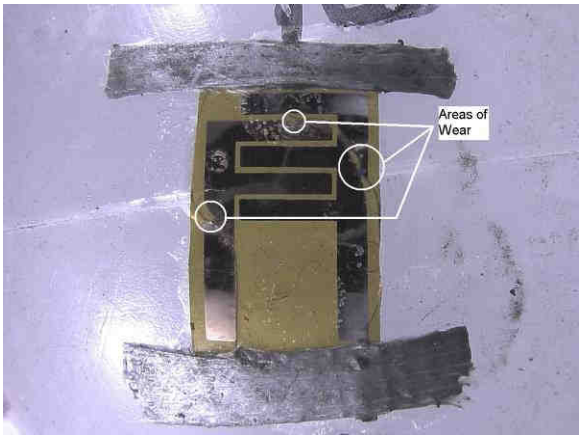

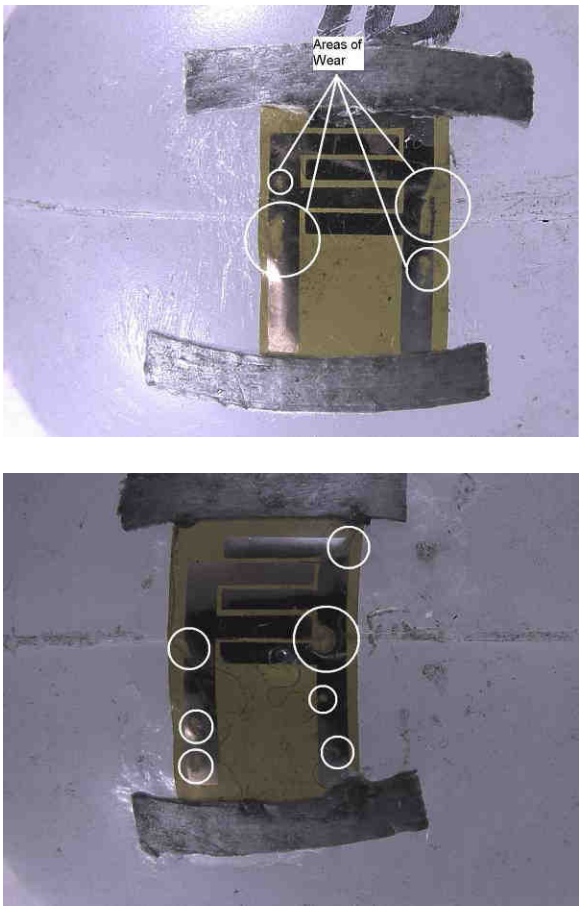

Figure 12: Images of sensors from durability test.

The test demonstrated that the sensors are susceptible to considerable amounts of wear from the inner pipe environment if left unprotected. Though the process of adhering the sensors to the ball was somewhat tedious, the sensors did not peel off during the test. The adhesive interface between the ball and the sensor did not interfere with the durability of the sensors in this configuration.

Based on these findings, it is apparent that the face of the sensor will need to be shielded if these sensors are to remain functional during actual test runs. This cannot be achieved for the current spherical packages, as areas would need to be carved away which would weaken the package, making it susceptible to crushing under the high pressures inside the pipeline. Therefore, it was conceived to mold the package, either as a solid unit (a casting), or as a shell around the existing sphere. The molding would serve two purposes; first, to strengthen the spherical package, and second, to allow for recessed areas to be molded in the shell itself.

3.2.2 Solid Spherical Packaging

To understand the feasibility of a pourable package, two approaches were taken. The first was to fill a hollow sphere with epoxy to determine the weight of such a package, and whether such a thick "casting" of epoxy would cure to proper strength. The second approach was to mold the epoxy around an existing hollow sphere to see if it would cure to form a suitable shell.

The solid epoxy form was made by pouring Aremco-Bond 2300 epoxy into a 2.5" spherical mold (cast solid). The shell form was made by pouring the epoxy into the same mold, but a 2" hollow sphere was inserted into the mold as a core (molded hollow). The intent was to get the epoxy to flow around the sphere, and then cure into a "nested" spherical package. This approach was also modified by adding 1 cm square pieces of PS to the mold (recessed hollow) to determine if a recessed area could be included in the nested spherical package. An image containing specimens from all three procedures are shown in Figure 13.

The moldings shown appear incomplete due to the inclusion of voids from air bubbles. Strategies to overcome this will be attempted in the second quarter of this project by including risers in the mold design, which will counteract shrinkage and alleviate void formation in the cured product.

The cast solid method was found to yield a robust resultant package. The solid aspect of the package meant it would withstand the high pressures of the pipeline, but the package weighed over 100 grams. The density of the solid package is too high for fluidized purposes. A solid epoxy sphere that weighed 30 grams would only have a 0.85" diameter, which is smaller than the electronics that need to be encased by the package.

Figure 13: Images of specimens from each molding method.

The solid package concept could be expanded upon by using filler materials such as foam to "take up space" in the volume of the package at a much reduced weight. This approach, however, was not readily feasible and was abandoned.

The poured shell concept was examined in a number of iterations. Great difficulty was encountered in forming this mold as the epoxy used was of its high viscosity (5000 cps). The poured epoxy also needs to replace air in the mold, which was difficult as the mold was rather tight in the radial direction between the core and mold wall. Although the cured epoxy was of adequate strength, and bonded well with the inner sphere, the shell was incomplete due to voids from trapped air bubbles. The voids result in weak points in the shell, and the epoxy surrounding the void often cracked upon removal from the mold.

The concept of having a poured package for these sensors was demonstrated in a number of methods. For the poured shell method to become feasible, a more flowable epoxy-type compound will need to be used. For this, a urethane elastomer compound with viscosity of 1100 cps was ordered. The relatively lower viscosity should allow for easier molding, and the elastomeric qualities should reduce the cracking of the shell around the inner sphere. These efforts along with mechanical testing of the packages will be performed and evaluated in the second quarter. In addition, the weight constraint (< 30 g) of the final package continues to be a challenge.

3.2.3 Hollow Package Designs

For the hollow spheres, the critical pressure for imploding the sphere can be roughly calculated using Eq. 1 (ignoring asymmetric pressures, buckling, and any prior defect).

$$\sigma_c = \frac{P * r}{2t} \qquad [1]$$

Although the failure pressure could be calculated using more sophisticated methods, for designing the packaging this was considered sufficient. Pressure testing was considered more expedient for evaluating the actual critical pressures of the spheres. Values of σc for some selected polymers are listed below.

Polypropylene (PP) –	7,000 psi
Acrylic -	15,000 psi
Epoxy -	20,300 psi
Polyester -	20,000 psi

As we were limited to purchasing an off-the-shelf solution, several vendors were queried and the following products were discovered.

1. Polypropylene Spheres with t = 1/16” with 1.5 and 2” diameters.
2. Acrylic Spheres with t=3/32” with 1.5”, 1.75”, and 2” diameters.
3. Low-viscosity (pourable) epoxy.

Each of the identified products was purchased. An off-the-shelf sphere could be bisected, the sensor and mote electronics inserted, and then reconnected with an epoxy adhesive for a spherical base package. Although the 1.5” spheres do not have enough enclosed volume to house the electronics, they were purchased to better understand how the packaging schemes behaved in the high pressure environment. Also, in the eventual miniaturization of the electronics, these packages would be possible choices for sensor packages.

3.2.3.1 Off the Shelf Hollow Spheres

To determine how the different products behaved, each of the PP spheres and the 1.75” Acrylic sphere were placed individually into an autoclave. The acrylic sphere came as two hemispheres, which were adhered together around the equator with epoxy to form a uniform sphere. The pressure in the autoclave was slowly raised to 2000 psi to determine the maximum pressure withstood by each option. All of the spheres failed at less than 2,000 psi. A comparison of the calculated critical pressure (Eq. 1) and the Actual Failure pressure is shown in Figure 14.

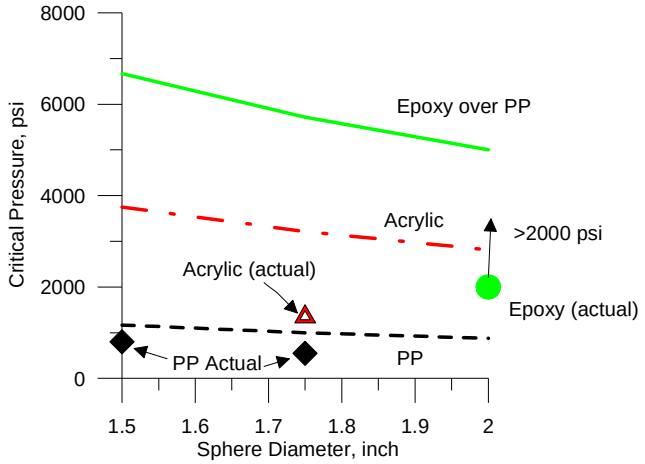

Figure 14. Comparison of calculated vs. actual failure pressures of different spheres

Of the two off-the-shelf hollow sphere, the acrylic sphere withstood the most external pressure, fracturing at 1350 psi. The shattered sphere did not appear to fracture at the seam, indicating the epoxy adhesive was not the "weak point" of the package. The mass of this package was measured at 15 grams. Neither of the PP packages was able to withstand 1.5 times the nominal pressures of a pipeline environment (about 1000 psi). Of the two, the 1.5" ball shattered upon failure, while the 2" ball showed more ductility and folded under the pressure. Either situation would be catastrophic to the inner-electronics and unacceptable for introduction to a pressurized pipe in the off-the-shelf condition. In all cases, the actual failure pressure was significantly lower than that calculated using Eq. 1, which is not surprising.

3.2.3.2 Cast Epoxy Shell Spheres

In order to determine if the bare spheres could be fortified, an epoxy shell was cast around the 2" PP sphere. Two castings were prepared. The first was a one-step casting that resulted in an off-centered casting as the hollow core floated before the epoxy set. This yielded a 1/32" shell on one side of the sphere, and a 7/32" shell on the other. The second rendition yielded a centered casting, with an approximately uniform 1/8" casting around the sphere. The uniformity was achieved by casting the shell in two parts. The first cast was done while the PP sphere was centered and held in the mold, and the second to complete the shell after the first had set. The 1/8" sphere is shown in Figure 15, after it was subjected to the autoclave high pressure tests.

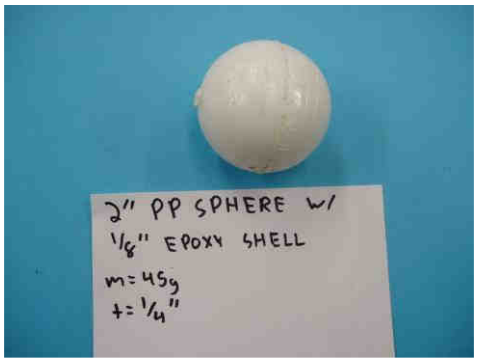

Figure 15: Image of the pressure tested epoxy cast spherical package, 1/8" wall.

The 1/32” off-centered shell was found to fracture at 2,000 psi, while the uniform 1/8” casting did not fracture in the test (Max. Pressure > 2,000 psi). Casting an epoxy shell around the PP sphere was found to fortify the PP spheres in both cases. In addition, the shell also provides a method to accommodate recesses for the sensors in order to protect them from the pipe wall, a necessity for a working package (see previous report on wear testing of sensors). However, the casting procedure results in varied thickness and strengths of the fortified package (the off-centered casting), and adds significant mass to the package to the point where it would negatively affect the flow characteristics of the package. Irreproducibility of this fabrication process makes it a poor candidate for creating pressure vessels.

3.2.3.3 Spheres with Recessed Shells

For the base sphere or core of the package which would house the electronics, the 1.75” acrylic sphere was selected. The sphere was able to withstand 1350 psi, which is strong enough to survive most pipeline environments, and weighed less than 20 g. The packaging scheme of a base sphere needs to be appended to include methods to recess the sensors. As the base sphere needs to retain its wall thickness, no machining of the acrylic sphere to recess the sensors could be performed. Instead, the recesses could follow two schemes. First, the 1.75” sphere could be nested in a 2” sphere. The 2” sphere could then be bored out over the sensors, resulting in a window where the sensor would be able to access the pipeline environment as it flowed by. Second, the “windows” could be made in an epoxy cast by placing a blank form over the sensors, casting the epoxy, then removing the forms in the demolding process.

For the first scheme, the 1.75” acrylic was placed in both an acrylic and a PP sphere. These packages are shown in Figure 16. Both of these would work in regards to recessing the sensors, but the added mass of a second acrylic sphere makes the scheme too heavy. The PP sphere however, adds only a few grams to the package for a total mass of 24 g. Both of these will withstand the same pressures as the 1.75” acrylic sphere alone, as this remains the load bearing portion of the package.

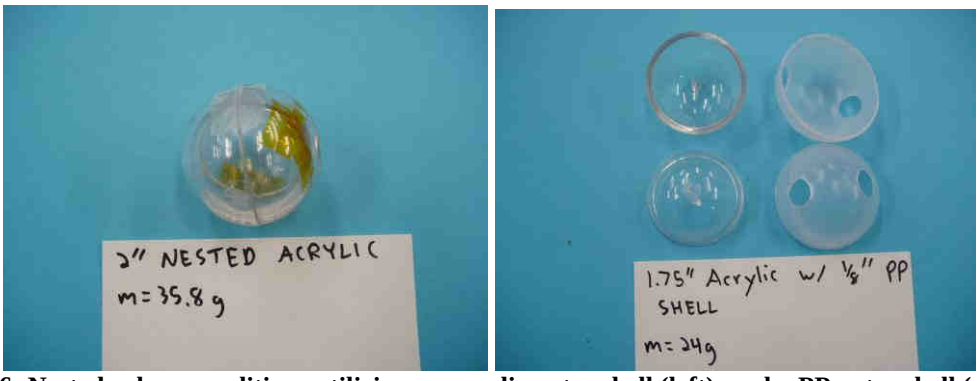

Figure 16: Nested sphere renditions utilizing an acrylic outer shell (left), and a PP outer shell (right – in deconstructed form).

Of the packaging schemes tested, the acrylic sphere was selected as the best candidate for the core of the sensor package. The other packaging schemes tested were either too heavy to promote adequate flow of the sensor, or too weak to withstand the inner-pipe environment. The acrylic sphere itself is inadequate to protect the corrosion sensors from wear, so methods to append the sphere with an outer sphere having ports to allow sensor access to the pipeline environment. Of the schemes tested, the 2" PP sphere was selected as the best as it could be easily adapted to the acrylic sphere, and added the least amount of mass to the base package. Therefore, the packaging scheme for the fluidized sensors will consist of a 1.75" acrylic sphere which will house the electronics, and fitted with a 2" PP shell having ports where the corrosion sensors will be situated. The combined mass of this package was measured to be 24 g, which is slightly higher than the 20 g target, but was the best possible package created from off-the-shelf components. Despite the 24 g mass, the assembled package is still expected to weigh less than 40 g, which should be light enough for adequate flow according to the flow modeling calculations performed to date.

3.2.4 Creep Testing of Nested Sphere Packaging Scheme

The mechanical testing of packaging reported last quarter focused on rapid failure due to pressure increase and did not evaluate longer-term creep and rupture. As the completed packages would have to withstand the high pressure environment of a gas pipeline for several hours/days without failing, the packaging schemes were tested by pressurizing to 1000 psi and holding this pressure for approximately 12 hours. The pressure was then reduced, and the packages inspected for damage.

The bare acrylic sphere was subjected to static 1000 psi loads and found to fail within 15 minutes in these pressures. The same packages shattered at pressures of 1350 psi when pressurized dynamically. It appears the time-dependent failure at lower pressures will be a more stringent requirement to fulfill for the sensor packaging.

As the bare acrylic sphere fractured quickly at 1000 psi, the nested packaging scheme may be able to reinforce the inner acrylic sphere. For this to occur, a strong bond between the inner and outer spheres is needed. To achieve this, a solvent based adhesive, or "polymer weld" was obtained. This adhesive lightly dissolves the surface of the polymer it is adhering to so that when it cures, a seamless interface is established. These packages were found to fracture within 12 hours. The fractured packaged showed that delamination of the inner-sphere from the PP occurred, indicating that the polymer weld did not seem to adhere well to the PP material. The solvent based adhesive did seem to toughen the acrylic, however, as the acrylic did not shatter but rather deformed plastically as shown in Figure 17.

Figure 17: Plastically deformed Acrylic sphere with PP outer sphere.

In lieu of the solvent based adhesive, a nested sphere design was fabricated with an epoxy filler to bond the two spheres. These packages also fractured within 12 hours of exposure to 1000 psi. The epoxy did not toughen the inner sphere, so the fracture mode returned to brittle, as can be seen in Figure 2.

Figure 18: Epoxy filled PP outer sphere fractured packages.

Since the polymer weld did not seem to adhere to the PP, an acrylic outer sphere was utilized to determine if this could strengthen the sensor packaging when intimately bonded to the inner sphere. This scheme did not fail at 2000 psi, nor was it found to fail within 12 hours at 1000 psi. Some deformation of the spherical package was noted, and is shown in Figure 19.

Figure 19: Nested acrylic spheres pressure tested package.

The deformation occurred around one of the outer-sphere recesses, an area expected to be a weak point for the package. The recesses tested here were ½" in diameter. Current testing is evaluating a similar packaging scheme with 3/8" recesses. The smaller recess should not weaken the package as much, resulting in less overall deformation.

3.3 Sensor Design, Location and Communications

Sensor integration and assembly consisted of several parallel activities related to the overall component integration, sensor location methods and electronics, and the communications methodologies and protocols. The sensor design schematics and fabrication layout drawings are included below.

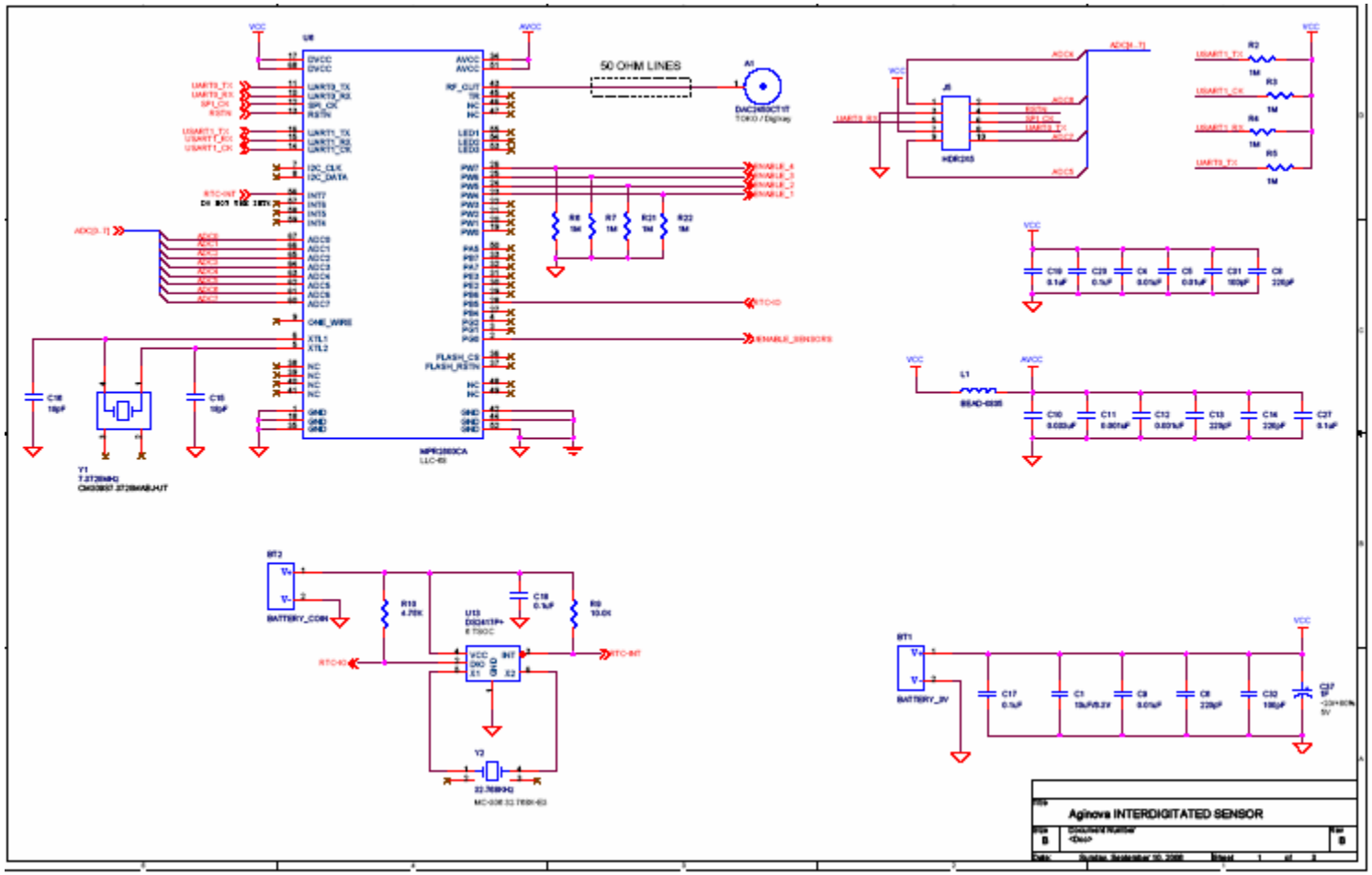

Figure 20: Sensor electronics schematic.

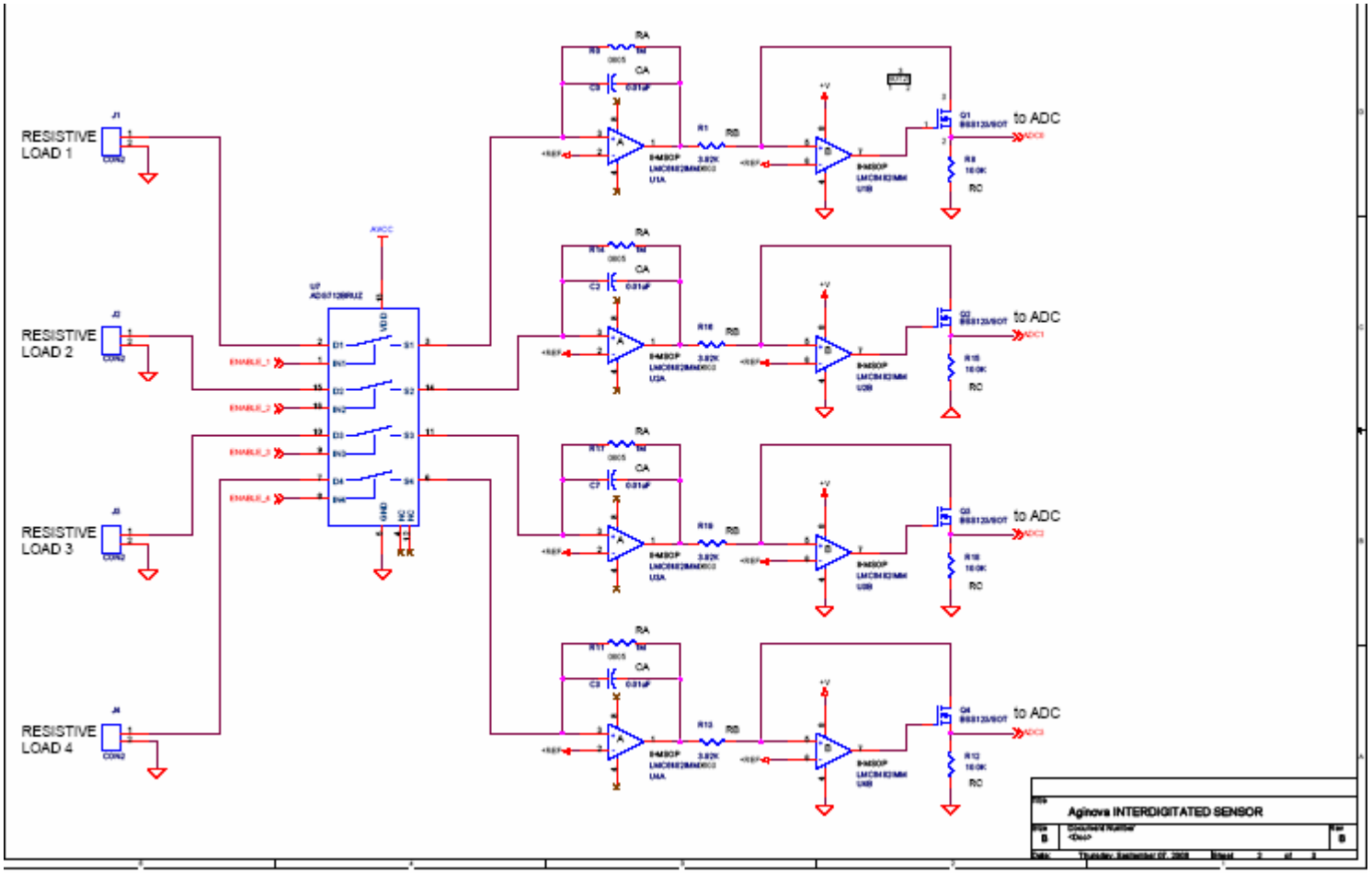

Figure 21: Sensor electronics schematic.

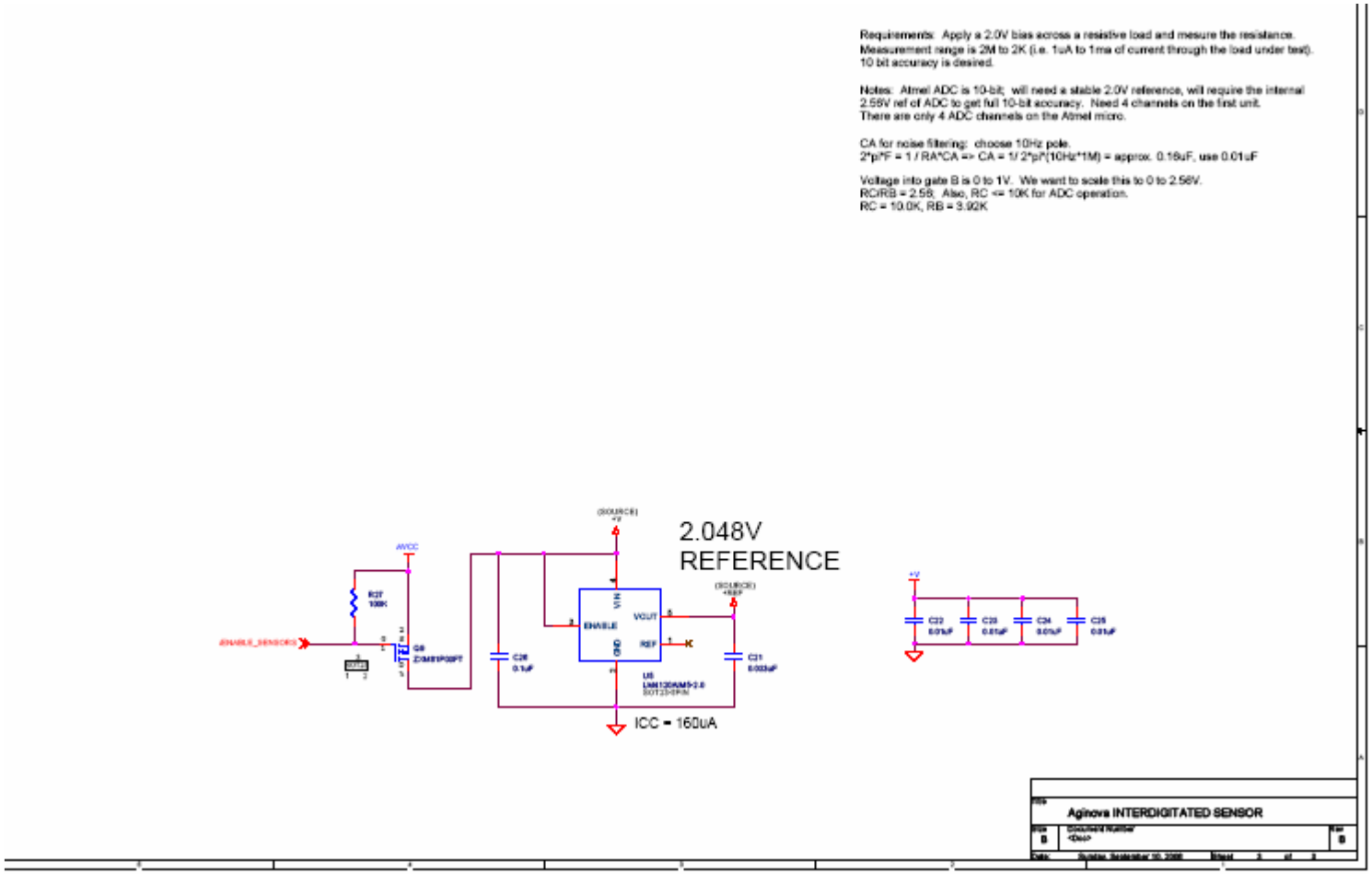

Figure 22: Sensor electronics schematic.

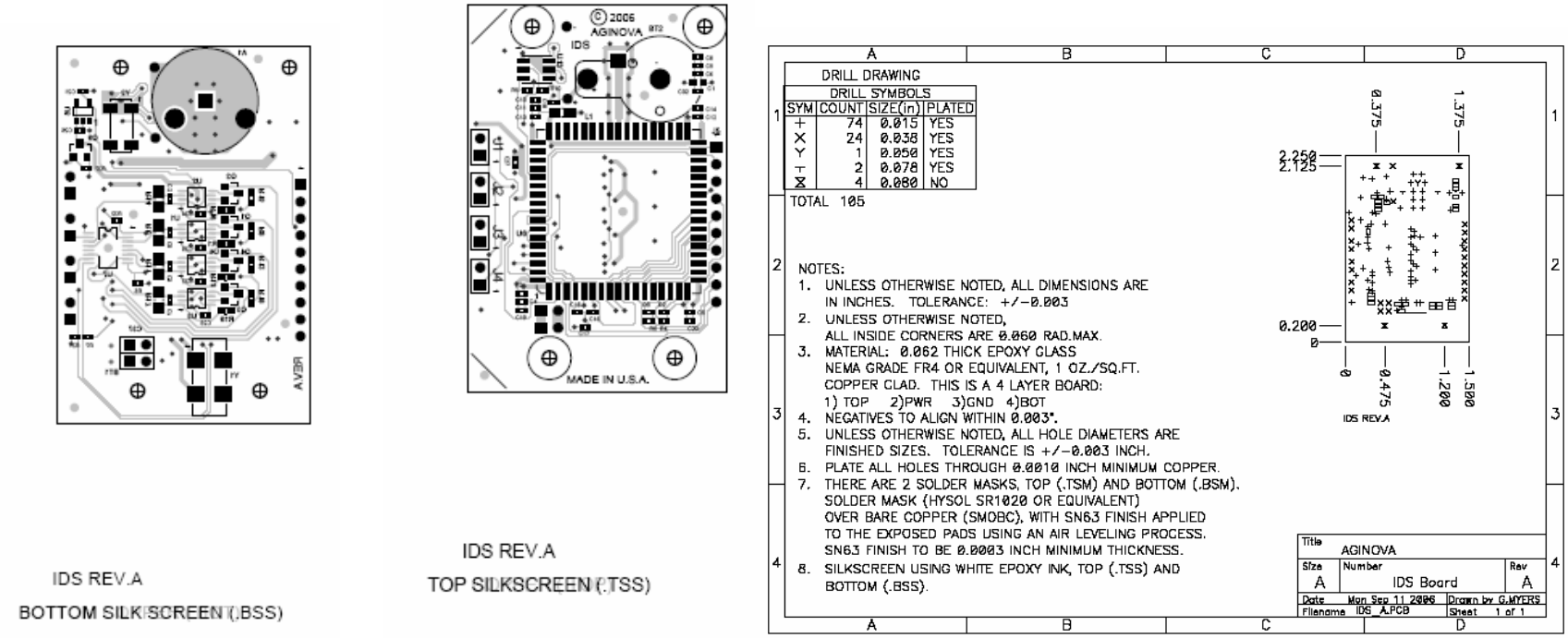

Figure 23: Sensor fabrication layout schematics.

3.3.1 Sensor Location Tracking

The methodology that has been adopted consists of a spherical ball with the packaged mote inside that rolls inside the pipe using the air pressure in the pipe. As the sensor ball rolls, it makes various measurements inside the pipeline. The measurements are stored locally at the sensor mote inside the ball. When the ball exits the pipe, the data is uploaded into the data analysis system which then reports the location inside the pipe where corrosion has been detected. For example in the figure below the ball rolls along the pipe in the direction of the air flow (the arrow).

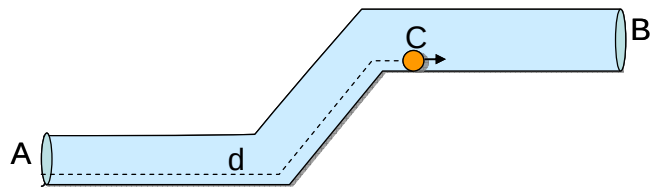

As the sensors in the ball are making the reading they are stored locally in the mote flash memory. Each measurement is time stamped using a local clock that is synchronized with an external clock source. A critical piece of information is the location of the ball inside the pipe. The location may be just the distance d from the starting point of the pipe or it may be the (latitude, longitude) coordinates of the position. In general, the positional accuracy needed is within a few feet.

Several methods were explored to provide this location information including time domain reflectometry, acoustic ranging, optical translation measurement, ultra-wide band communications, and time of flight calculations. Each of these is discussed below.

3.3.1.1 Time Domain Reflectometry

Time domain reflectometry (TDR) has been used extensively in the measurement of distance along coaxial cables. An electromagnetic wave that propagates along the Cable will be reflected by breaks and faults in the cable. By detecting the echo and measuring the difference in time of arrival we can estimate the distance to the fault. Such a methodology can be modified for measuring distance inside the pipe. A transducer at A sends a RF pulse towards B which is heard by the mote at C. When the mote hears the pulse it responds with an acknowledgement pulse. The receiver at A hears the response pulse and calculates the distance d. Since the pipe is metallic, the RF wave propagates in the cylinder waveguide and can travel a long distance with little attenuation. This type of micro-radar is operationally complex but elegant. The methodology to compute the distance inside pipelines is novel and has not been attempted before. With novelty comes the added risk of uncertainty of the entire methodology's feasibility.

After some initial feasibility studies, this approach was abandoned.

3.3.1.2 Acoustic Ranging

Similar to the radar principle of the TDR methodology we can make measurements by using a sonar principle with audio waves. An audio source at the mouth of the pipeline (A) generates audio pulses that are detected by the sensor (microphone) at B. By knowing the speed of sound and using synchronized clocks we can estimate the distance from A to B. The audio scheme avoids all issues related to the round-trip time based methods by relying on the synchronized clocks and the knowledge about the speed of sound. However, there are some issues to be resolved with respect to multipath transmissions.

The audio waves in the pipe will be planar waves depending on the frequency of the source. Approximately we estimate that planar waves will be generated inside the pipe for frequencies below 500Hz. It is usually a challenge to generate an audio source at such low frequencies. But since the transducer will stay outside the pipe the size will not be an issue. Since sound propagates through the pipe exterior we can develop a transducer that couples with the pipe from the outside.

To address the multipath problem we could depend on the transmission of the sound through the metal of the pipe instead of the air inside the pipe. Sound will travel faster through the metal. By detecting the first impulse and rejecting all the subsequent echoes, we will be able to accurately time the generation and reception of the sound. Calibration of the distance computation will have to be done for each pipeline at the site. However, this is not too difficult as it can be done by placing sensors at the outside of the pipe at known distances. The methodology to compute the distance inside pipelines using AR is novel and has not been attempted before. With novelty comes the added risk of uncertainty of the entire methodology's feasibility.

Further study ruled out this approach for gas pipelines but is now being explored for possible use in liquid petroleum pipelines.

3.3.1.3 Optical Translation Measurement

The optical computer mouse uses an optical system based on lasers and detectors to accurately record the translations in x and y directions of the mouse. The optical translation measurement (OTM) system for distance computation inside the pipeline uses this principle to compute the position of the mote inside the pipeline. The methodology to compute the distance inside pipelines using OTM is novel and has not been attempted before. With novelty comes the added risk of uncertainty of the entire methodology's feasibility. In general we viewed the OTM method as having higher risks than the AR or TDR methods and was not pursued further.

3.3.1.4 Ultra Wideband Ranging

Ultra wideband RF signals have been used in many radar type of applications. UWB transmitters are small and require a small amount of power while the receivers are more

complex. In the pipeline application this means that we can mount the UWB transmitter on the mote platform that moves down the pipe and have the complex and bigger receiver units at the end points of the pipe. Range computations will be based on relative time of arrival at two different receivers (or Time difference of arrival).

Because this approach initially looked attractive, a full UWB system was procured and its ability to track sensor location in a high pressure flow loop test was conducted. To perform this, ultra wideband radio frequency identification tags (UWB RFID) were evaluated. These tags have been designed to give three dimensional locations of assets in storage, allowing wireless identification and location of assets in a monitored space. For our purposes, we scaled this technology to a pipeline, which essentially acts as a 1-dimensional space so that the sensor can follow from the launch point to the collector. To accomplish this, ultra wideband radio frequency identification tag (UWB-RFID) asset tracking technology from Multi-Spectral Solutions was utilized. This technology performs time difference of arrival (TDOA) measurements of transmitted UWB signal from the fluidized sensor to receivers at each end of a pipe test section to calculate the location of the sensor. Individual components of this asset tracking technology are shown in Figure 24.

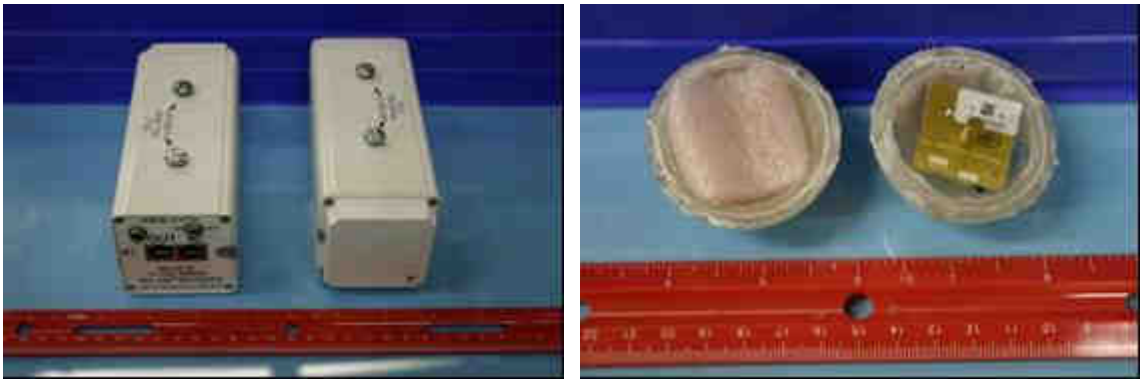

Figure 24: Receivers (left) and a UWB-RFID tag shown in a fluidized sensor package (right) used to perform sensor location tracking.

To implement this technology in pipeline applications, it was necessary to insert the respective components inside the piping, yet protect the components from the high pressure and potentially corrosive environments that exist in gas transmission pipelines. The UWB-RFID tag is enclosed in the fluidized sensor which protects it, but customized housing for the receivers was created. An image of the housings for the receivers are shown in Figure 25.

Figure 25: Protective housing for the UWB receiver.

To validate the UWB system, the average velocity of the ball was measured in two ways. For tests where only the time of flight was recorded, the length of the pipe was divided by the time it took the sensor to travel the pipe. For tests where UWB RFID technology was used to track the location of the packages as they flowed, the position in the pipe was plotted versus the time of position measurement, and the slope of this line taken to yield the average velocity. Using the latter approach, Figure 26 shows the position vs. time plots individually.

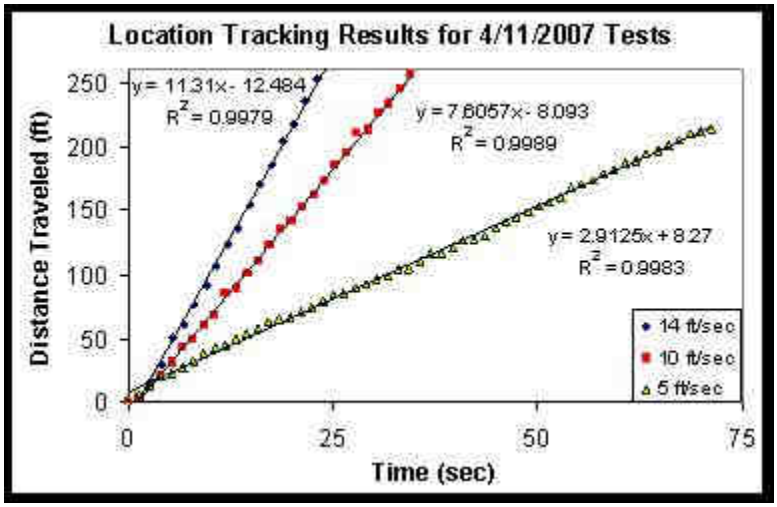

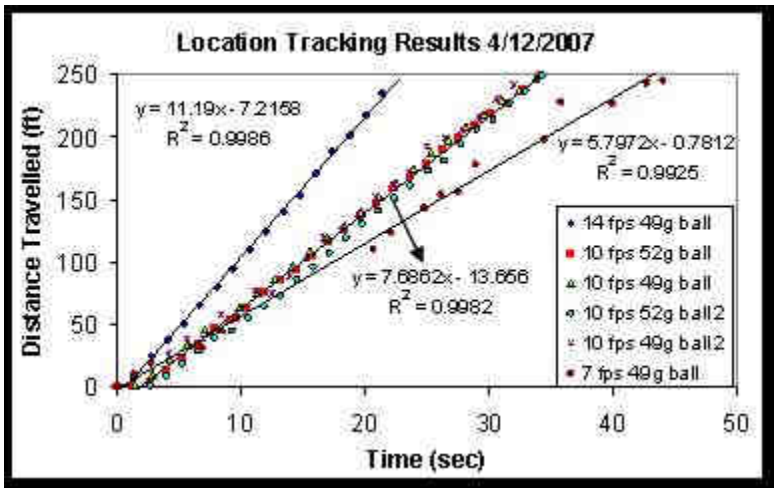

Figure 26: Position vs. time plots for sensors using UWB location tracking.

Combining the time of flight calculations with the location tracking calculations of velocity, Figure 27 plots the average ball velocity vs the gas velocity as observed for an approximately 50 g 2 in diameter ball at pressures of 750-900 psi in a 12” diameter pipe. The plot shows that the ball velocity tracks linearly with the gas velocity. Extrapolating the trend to the x-axis intercept indicates that the minimum flow velocity needed to move a 50 gram ball is 2 fps.

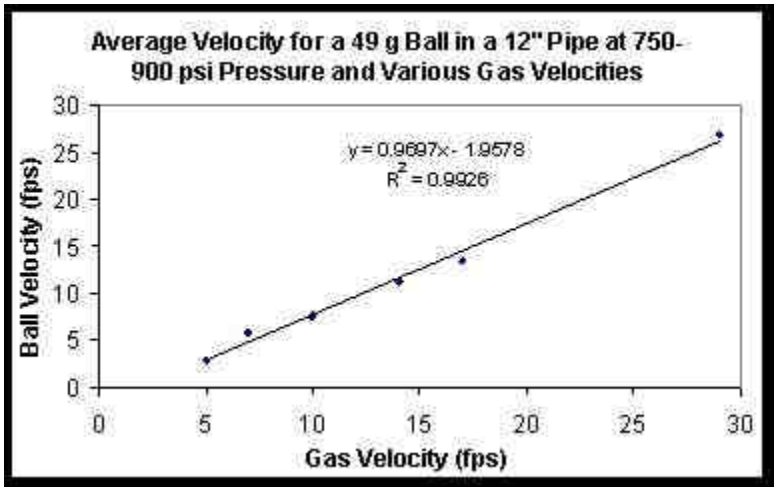

Figure 27: Ball flow velocity as a function of gas flow velocity at pressure in a 12” pipe

Though these results were very promising, over the course of the project, difficulties in adopting the UWB approach became apparent. These difficulties included incompatibilities

between different hardware and communications protocols and size and expense of the UWB units led the project team to consider other alternatives.

3.3.1.5 WiFi Mote Ranging

The challenges with adopting the UWB approach coupled with the technological development of WiFi based motes (Figure 28) precipitated a design change. WiFi-based systems have the advantage of being able to leverage existing wireless network systems in addition to creating their own network. This configuration has many advantages over the UWB approach especially for “leave in place” monitoring systems. One advantage is that a wireless equipped PDA (e.g., Palm, PocketPC) can send commands and receive data thereby simplifying the interface structure. Thus, though the UWB approach has been demonstrated and could be used under some circumstances, a WiFi version appears to be the optimal configuration.

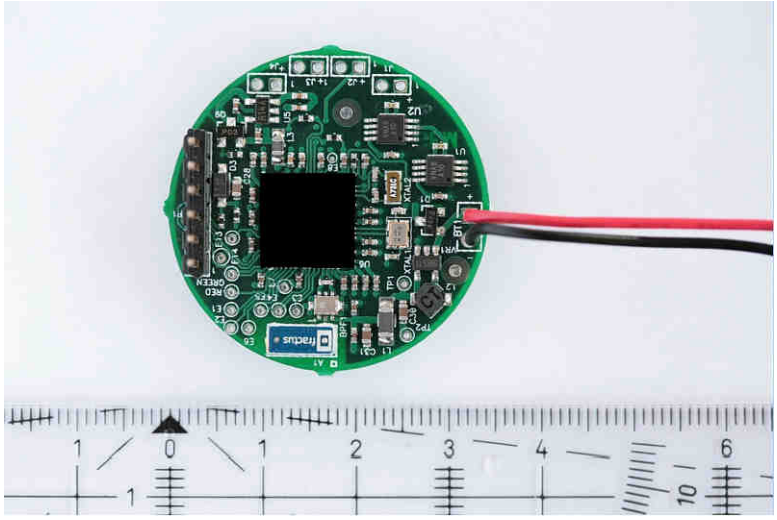

Figure 28: WiFi mote circuit. Scale shown is in centimeters.

The decision to move to a WiFi mote from the ZigBee mote demonstrated in Q2 FY07 was due to the need to have a field-deployable location tracking capability. The ZigBee communications standard would not allow an accurate means to do this, while WiFi is capable of tracking mote location through time difference of arrival (TDOA) calculations to within 10-15 feet.

The switch to the WiFi protocol instigated several unexpected challenges, as the WiFi protocol has required the implementation of a brand new chipset. In addition to the need for a new chipset, the new chipset requires a higher current burst than is obtainable with the primary Li-ion batteries used in the initial pilot demonstration. A suitable battery replacement was found, but this battery operates at 4V, and the chipset can only withstand a maximum of 3.6V. Therefore, a Voltage reducing diode was designed and implemented to interface between the battery and the chipset. A schematic of the diode modification is shown in Figure 29.

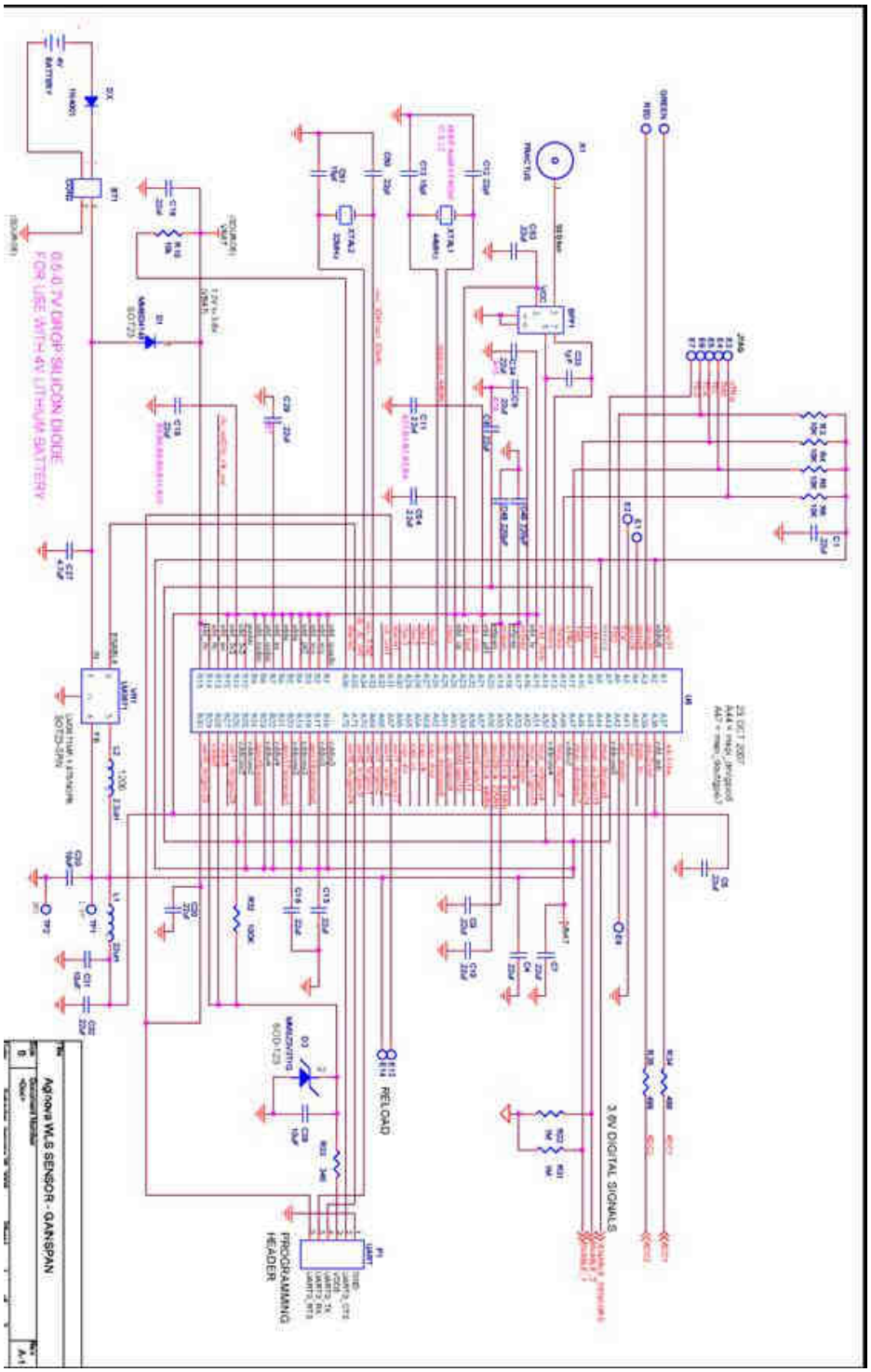

Figure 29: Schematic of Voltage Modified WiFi Fluidized Sensor Electronics

3.4 Sensor Injection and Retrieval Systems

The sensor injection and retrieval system design was composed of a pair of ball valves that allow introduction the sensors from ambient pressure into the higher pressure flow loop (shown schematically in Figure 30. The sensor retrieval system presently consists of a thin mesh inside a pipe tee (Figure 31) that will divert the sensor to drop into the tee without decreasing the overall gas flow rate significantly. Once the sensor is diverted into the tee it will eventually exit the loop either via a double ball valve arrangement similar to the injection system (shown in Figure 30).

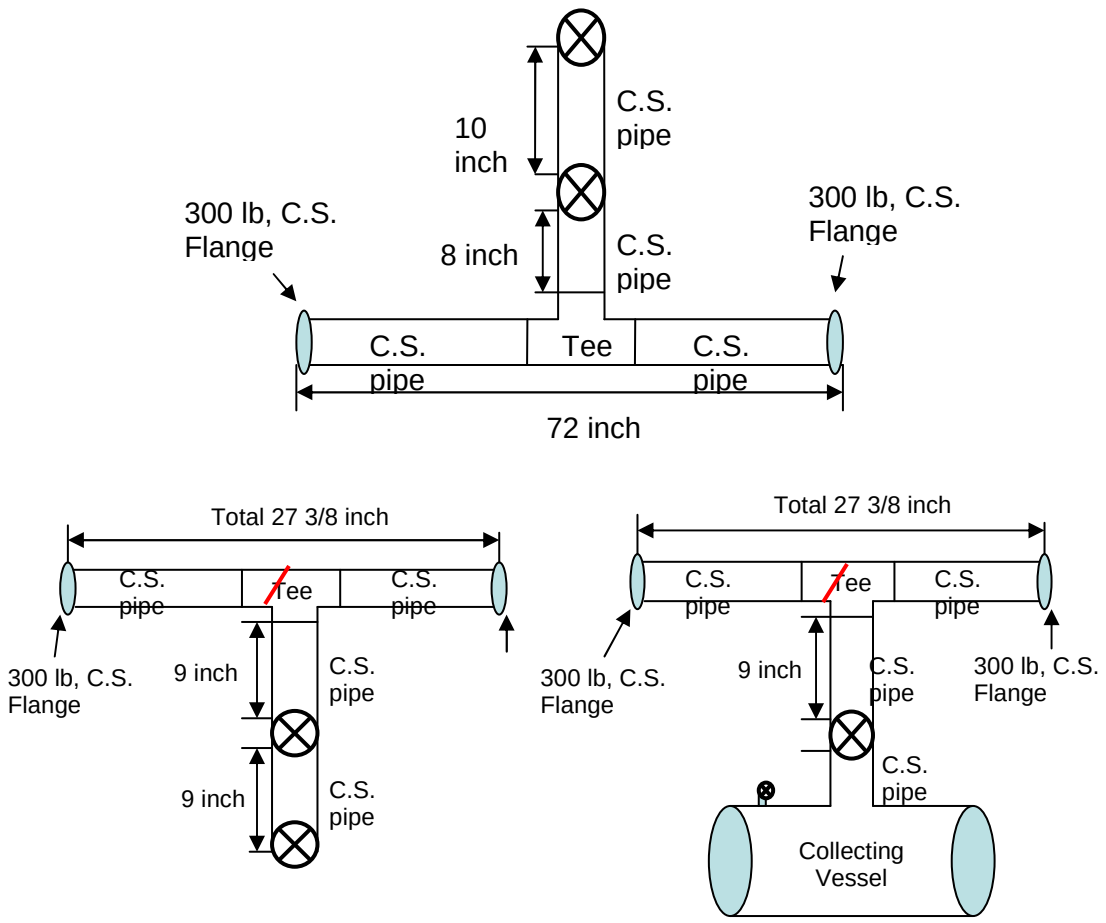

Figure 30: Schematic diagrams of sensor retrieval systems

Figure 31: Photographs of modified "tee" for injection and retrieval system

Systems similar in function and appearance to these have now been successfully used in several low pressure flow loop tests and in flow tests in higher diameter, high pressure lines.

3.5 Flow Loop Validation Trials

Several flow loop tests were carried out during the course of the project. The first was in a low pressure system to verify that the overall sensor concept using gas flow to propel the sensors was valid. The second flow loop test was conducted at higher pressures to help verify the UWB sensor tracking system (discussed previously). Two additional low pressure tests conducted under the guidance of pipeline operators were then conducted using fully functioning prototype sensor systems to validate the entire concept and to help promote industry awareness and acceptance of the technology.

3.5.1 Initial Low Pressure Loop Tests

The initial small diameter flow loop experiments were initially carried out at near ambient pressure in a 36-m long, 10.16-cm diameter loop. A schematic diagram of this system is shown in Figure 32 and shown photographically in Figure 33. Carbon dioxide gas was introduced into the system at an inlet pressure of 300 psi from a 6 ton storage tank. The flow rate of the gas was measured using a variable flow meter which had an operating range from 3 to 30 SCMM located between two ball valves.

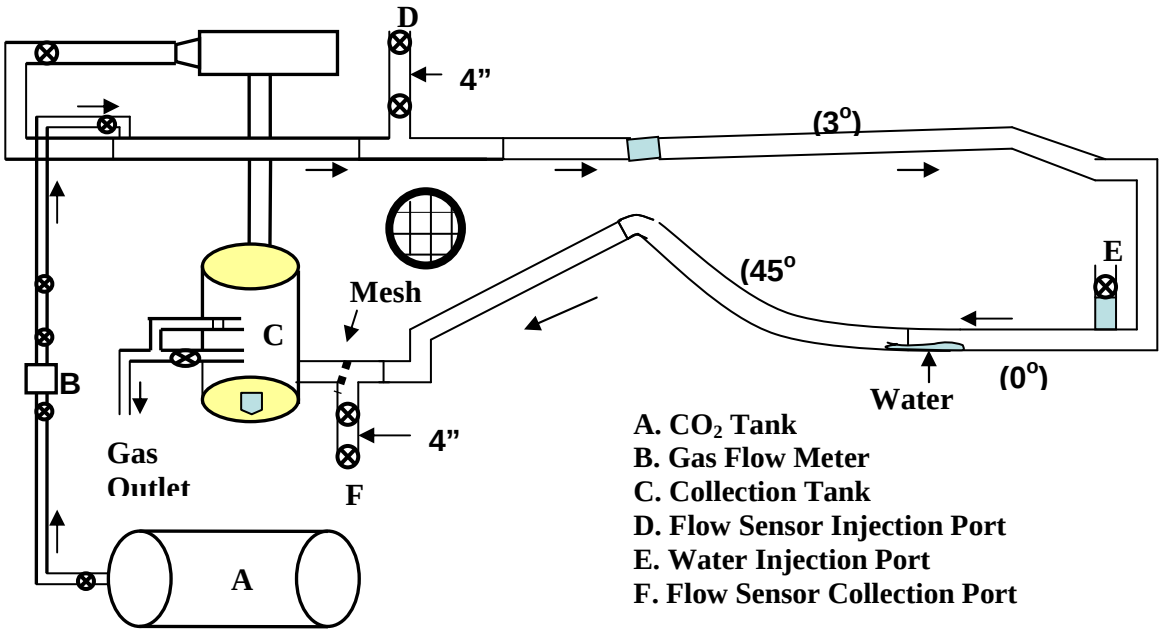

Figure 32: Schematic of flow loop system.

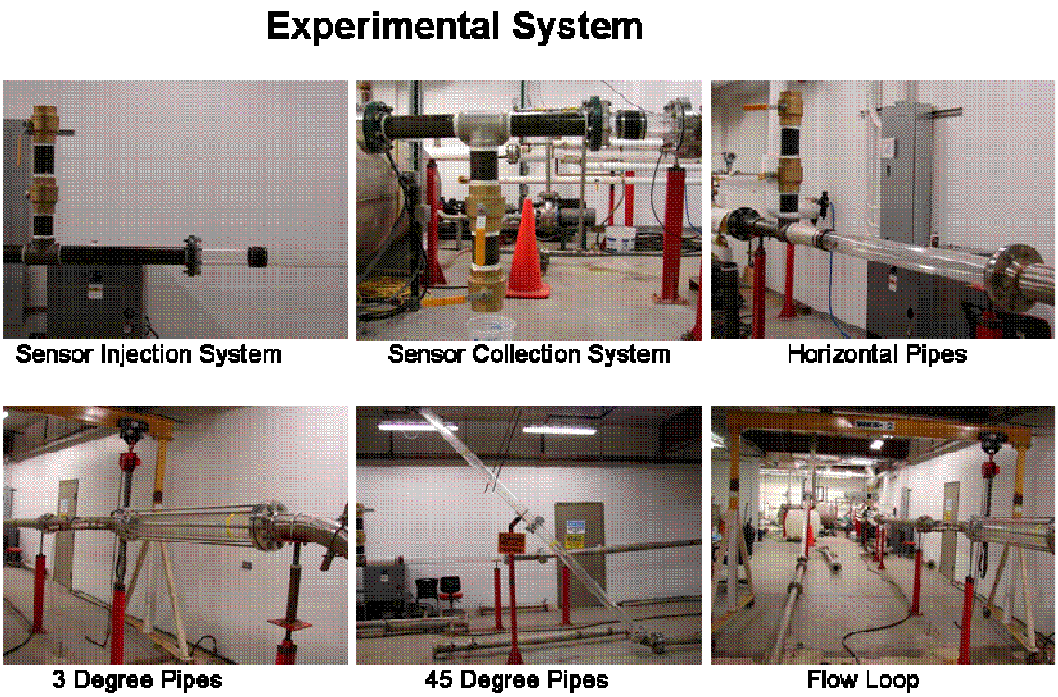

Figure 33: Flow loop system photos.

A summary of the results obtained is presented in Tables 1-3 and Figures 8-10 below. Results showed that sensor movement was highly dependent on sensor shape, weight balance, size, and pipeline inclination.

Table 1. Only one flow sensor in the pipeline ("motionless condition" refers to the sensor ball remaining stationary in the middle of the 45° incline section)

Sensor Weight	Gas Velocity Required for 0 - 3°	Gas Velocity Required for 45°	Observations
28.9 g	5 ~ 8 m/s	10.5 ~ 10.7 m/s	At a gas velocity of 9.9 m/s, sensor was "motionless condition" at 45 degrees.
27.2 g (Squeeze ball, 2.6 diameter)	2.7 ~ 3.3 m/s	6 m/s	At a gas velocity of 5.8 m/s, sensor was "motionless condition" at 45 degrees.
42.1 g	6 ~ 8 m/s	13.2 ~ 13.8 m/s	At a gas velocity of 12.5 m/s, sensor was "motionless condition" at 45 degrees.
42.1 g (Racquet ball, 2.19 diameter)	4.5 ~ 6 m/s	10.5 m/s	At a gas velocity of 10.2 m/s, sensor was "motionless condition" at 45 degrees.
51.7 g	7.0 ~ 9.2 m/s	13.9 ~ 15.0 m/s	At a gas velocity of 13.5 m/s, sensor was "motionless condition" at 45 degrees.
60.7 g	8.2 ~ 9.4 m/s	15.8 m/s	At a gas velocity of 15.0 m/s, sensor was "motionless condition" at 45 degrees.
73.3 g	7.7 ~ 10.3 m/s	16.7 ~ 17.2 m/s	At a gas velocity of 16.3 m/s, sensor was "motionless condition at 45 degrees. At 45 degrees, the sensor shows "sliding movement" (not rolling movement).

Table 2. Two sensors of similar weight in the pipeline ("motionless condition" refers to the sensor ball remaining stationary in the middle of the 45° incline section)

Sensor Weight	Gas Velocity Required for 0 - 3°	Gas Velocity Required for 45°	Observations
First, 28.6 g sensor was inserted and then 28.9 g sensor was inserted	11 m/s	11.5 m/s	Higher gas velocity was required at 0 and 3 degrees since two sensor contact together. 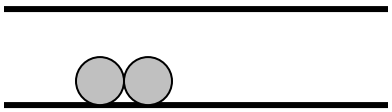
First, 28.9g sensor was inserted and then 28.6 g sensor inserted	10.7 m/s	11.0 m/s	Higher gas velocity was required at 0 and 3 degrees since two sensor contact together.
First, 42.1g sensor was inserted and then 42.4g sensor inserted	42.1g sensor moves at 6.0 m/s. 42.4g sensor moves at 8.5 m/s	42.1g of sensor: 13.5 m/s 42.4g of sensor: 14.0 m/s	Sensors moved separately.
First, 42.4g sensor was inserted and then 42.1g sensor inserted	Both sensors: 13.0 m/s	Both sensors: 14.0 m/s	Higher gas velocity was required to move sensors at 0 and 3 degrees.
First, 60.5g sensor was inserted and then 60.7g sensor inserted	60.5g sensor moves at 7.0 m/s. 60.7g sensor moves at 7.5 m/s	Both sensors: 15.9 m/s	At a gas velocity of 13.5 m/s, sensor was "motionless condition" at 45 degrees.

Table 2 Continued…

Sensor Weight	Gas Velocity Required for 0 - 3°	Gas Velocity Required for 45°	Observations
First, 60.7g of sensor was inserted and then 60. 5g	60.7g sensor moves at 8.5 m/s. 60. 5g sensor moves at 9.0 m/s	Both sensors: 16.0 m/s	Light sensor passed heavier sensor at 45 degrees. 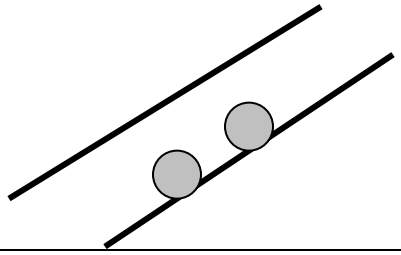

Table 3. Two different weight sensors in the pipeline

Sensor Weight	Gas Velocity Required for 0 - 3°	Gas Velocity Required for 45°	Observations
First, 28. 6 g of sensor was inserted and then 42.1 g of sensor was inserted. Initially, sensor locations are	28.6g sensor moves at 5.5 m/s. 42.1 g sensor moves at 6.0 m/s	Both sensors: 14 m/s	At 0 and 3 degrees, sensors moved separately. Before 45 degree elbow, two sensors stuck together. Therefore, higher gas velocity was required for movement. 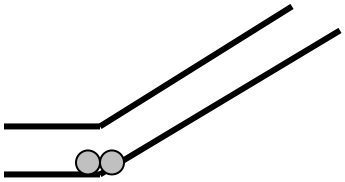
The same test was performed except a different location for sensors. The results showed that the gas velocity required at 0 and 3 degrees depends on location of sensors. However, similar results were seen at 45 degrees.			

Table 3 Continued ….

Sensor Weight	Gas Velocity Required for 0 - 3°	Gas Velocity Required for 45°	Observations
First, 28. 6 g sensor was inserted and then 42.1 g sensor was inserted. Initially, sensors location is 	28.6g sensor moves at 5.5 m/s. 42.1 g sensor moves at 6.0 m/s	Both sensors: 14 m/s	At 0 and 3 degrees, sensors moved separately. Before 45 degree elbow, two sensors stuck together. Therefore, higher gas velocity was required for movement. 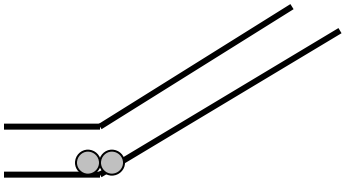
The same test was performed except a different location for sensors. The results showed that the gas velocity required at 0 and 3 degrees depends on location of sensors. However, similar results were seen at 45 degrees.			
Sensor Weight	**Gas Velocity Required for 0 - 3°**	**Gas Velocity Required for 45°**	**Observations**
First, 28. 6 g sensor was inserted and then 42.1 g sensor was inserted. Initially, sensors location is 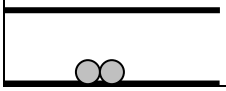	Both sensors: 10.5 m/s	Both sensors: 13.5 m/s	At 0 and 3 degrees, sensors moved separately. Before 45 degree elbow, two sensors stuck together. Therefore, higher gas velocity was required for movement.

			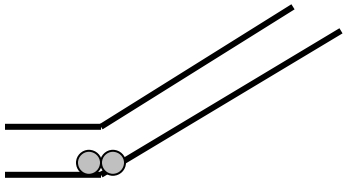

Table 3 Continued ….

Sensor Weight	Gas Velocity Required for 0 - 3°	Gas Velocity Required for 45°	Observations
First, 42.1 g sensor was inserted and then 28.6g sensor was inserted.	Both sensors: 6.0 m/s	Both sensors: 13.8 m/s	Sensors moved separately. Light sensor passed heavier sensor at 45 degrees.
Four different sensors were inserted at the same time. Insertion sequence: (#1) 73.2836g, (#2) 51.6551g, (#3) 42.0900g, (#4) 28.5936g A gas velocity of 14 m/s: #2, #3 and #4 sensors moved in 45 degrees. However, #1 sensor did not move to the 45 degree inclination. This means that lighter sensors passed heavier sensor.			

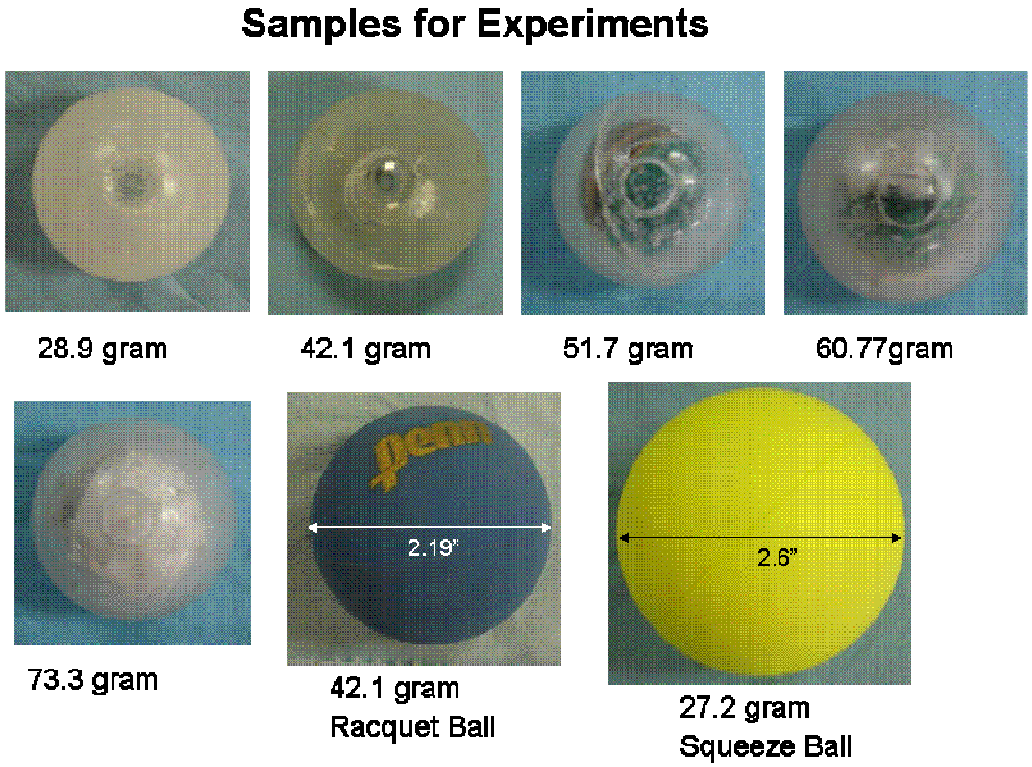

Figure 34: Photographs of mock sensors and alternate spherical objects used for flow testing.

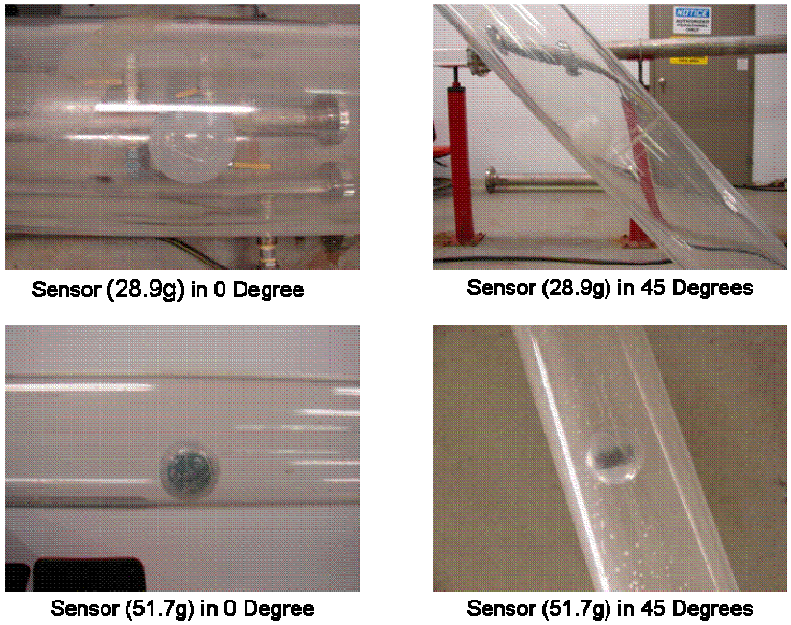

Figure 35 Photographs of mock sensors in clear pipe sections during flow loop testing

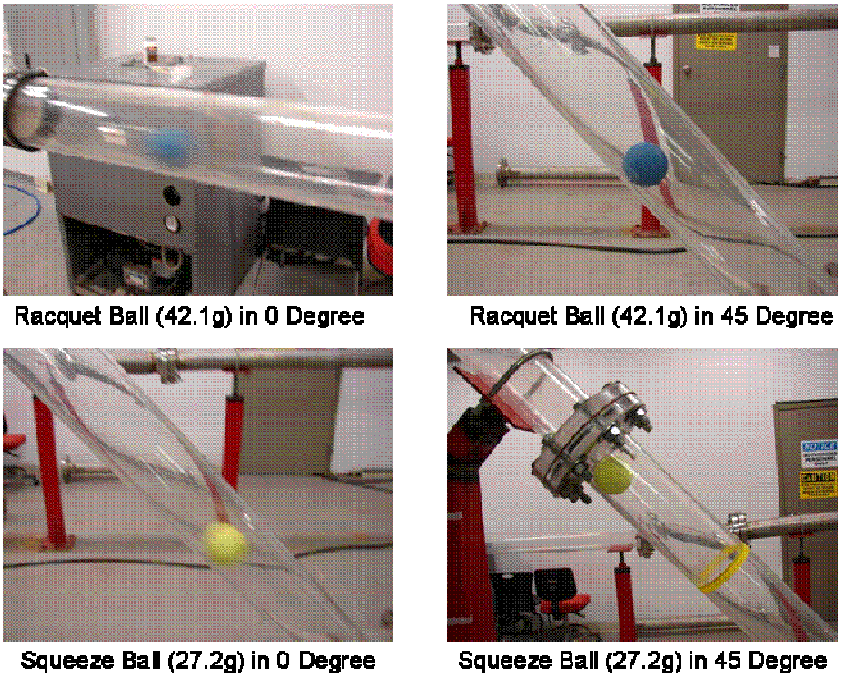

Figure 36: Photographs of alternate spherical objects in clear pipe sections during flow loop testing

3.5.2 High Pressure Flow Loop Tests

Implementation of a fully pressurized (900 psi) flow loop test of the sensor packages required the fabrication of several customized pipe sections (Figure 37). These customized sections allow the introduction into and retrieval out of the high-pressure gas stream through the use of an airlock compartment, the insertion of the UWB antennae to access the inner-pipe environment, yet protect the antennae from the high-pressure environment (antennae enclosure).

It was also necessary to fabricate a “launcher” apparatus and a “collector” apparatus to introduce the sensors into the pressurized gas stream from the outside environment, as well as extract them from the pipeline at the opposite end of the test section. Schematic illustrations of the launcher and collector, as well as images of the actual apparatus’ are shown in Figure 38.

With this set-up, the ball movement was tracked as a function of gas velocity at pressures ranging from 750-900 psi. Sensor movement was tracked by recording the time it took to travel the length of the pipe to get an average velocity, as well as by recording the location of the sensor through UWB RFID technology as a function of time as it flowed through the pipe. Results from these tests were presented previously with the UWB discussion.

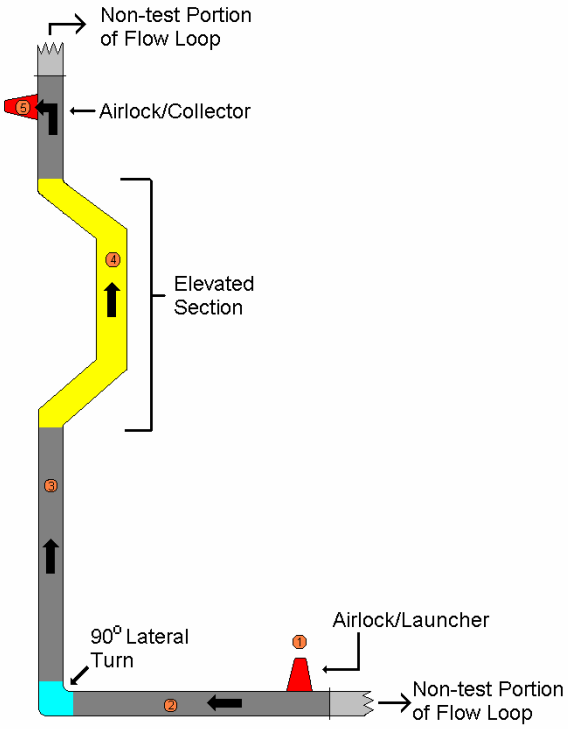

Figure 37: Schematic Top view of high-pressure flow loop at SwRI.

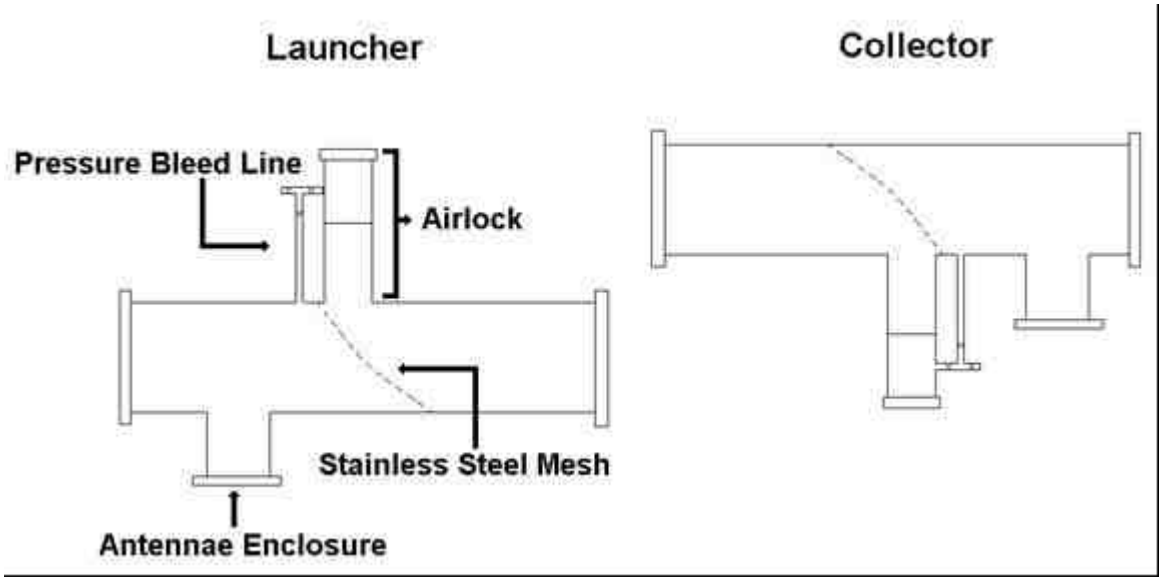

Figure 38: Schematic illustrations (top) and actual images (bottom) of the launcher (left) and collector (right) custom fabricated for administration of fluidized sensor testing.

3.5.3 Flow Loop Sensor Validation Trials

With the single functioning sensor, a successful flow loop trial was conducted with initial participation by DOT-PHMSA, BP and Dominion and a second flow loop trial with multiple sensors with participation by DOT-PHMSA, BP, ExxonMobil, Panhandle Pipeline were conducted. A schematic of the flow loop was shown in Figure 32. In the flow loop test, we demonstrated a fully functional prototype sensor system. In this test we showed that the sensor system could distinguish between dry gas, accumulated water, and water of different corrosivity (salt water vs tap water) with about a 1-2 second response time. Some data from just one of the sensor pads on one sensor ball is in Figure 39 below for illustration. We also successfully demonstrated the wireless communications platform. Due to the short length of the flow loop (only about 75 feet) we were not able to fully demonstrate the location aspects. Based on the feedback from BP and Dominion, there is support to keep moving forward with the technology; however several questions were raised (e.g., if the sensor encounters liquid petroleum, how quickly can it then detect water?). Before we could address these questions, we experienced an electronics failure in the first test.

After we recovered the sensor from the flow loop, we discovered that the main joint that holds to two halves of the sphere together failed resulting in water leaking into the sensor electronics. The epoxy used has worked in the past, however we only allowed 5 minutes of curing time instead of 24 hours.

A second round of flow loop tests was then conducted using multiple sensor balls. The results from using these sensors in multiple sequential runs is shown in Figure 42 - Figure 45. These tests were able to conclusively demonstrate that the sensors could operation through sequential runs and give similar results. In addition, water detection along slight slope inclines was also achieved. Attempts were also undertaken to reproduce the sensitivity to water chemistry (corrosivity) changes that were demonstrated successfully in the previous flow loop validation

trial. Based on the results obtained, it became evident that in the “once through” configuration where the sensor ball flows through the pipe at a relatively high rate of speed this is not possible. In order to provide detection of water accumulation (vs. dry gas) in the “once through” configuration, the data acquisition rate for the corrosivity sensor must be relatively high. That is, if the sensor is flowing in the pipeline the corrosivity sensor cannot be energized for a long enough period of time to obtain and accurate corrosivity measurement (which takes 1-2 seconds) and still be able to provide the spatial resolution along the pipe for water accumulation locating accuracy. Though this may sound like a limitation, the original idea of the “once through” sensor configuration was to just detect if any water accumulation had taken place at any location along the pipe. If no water was found, then no further analysis or inspection would be needed. If water accumulation was found, then additional inspection would be needed and might involve injection of the “leave in place” configuration sensor ball. The validity and ability of the “leave in place” configuration sensor ball to distinguish corrosivity differences was successfully demonstrated in the previous flow loop trial.

After successfully demonstrating that water that is smeared out along an incline could be detected, the sensors were then dipped in mineral oil to simulate the effects of prior liquid petroleum wetting on sensor performance. It was at this point that we encountered another sensor package failure. In this case, the mineral oil acted as a softening agent (solvent) for the epoxy that holds the thin film corrosivity sensors on the sensor ball (see Figure 40). This observation has identified another necessary design change related to the packaging. Instead of using epoxy to attach the thin film corrosivity sensors to the inner concentric sphere, a new corrosivity sensor head will be constructed using printed circuit board processes that will enable the insertion of these sensors in the form of a thin disk into the recesses located in the outer package sphere. This change should improve the overall integrity of the systems and should eliminate the reliance on epoxies for mechanical and sealing.

Upon completion of the second flow loop validation tests, the project team met with the pipeline operators present for feedback and suggestions on improvements and how to go forward. These recommendations are included in the Conclusions and Technology Implementation section below.

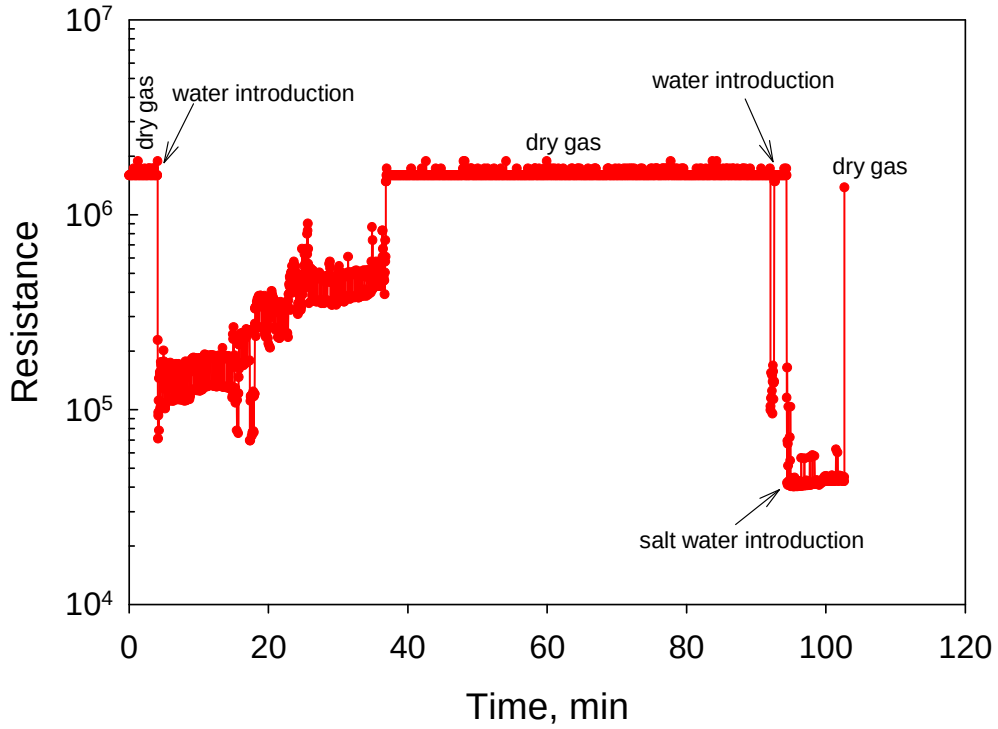

Figure 39: Initial results from first flow loop trial demonstrating that the sensor can distinguish between dry gas, entrained water, and entrained salt water.

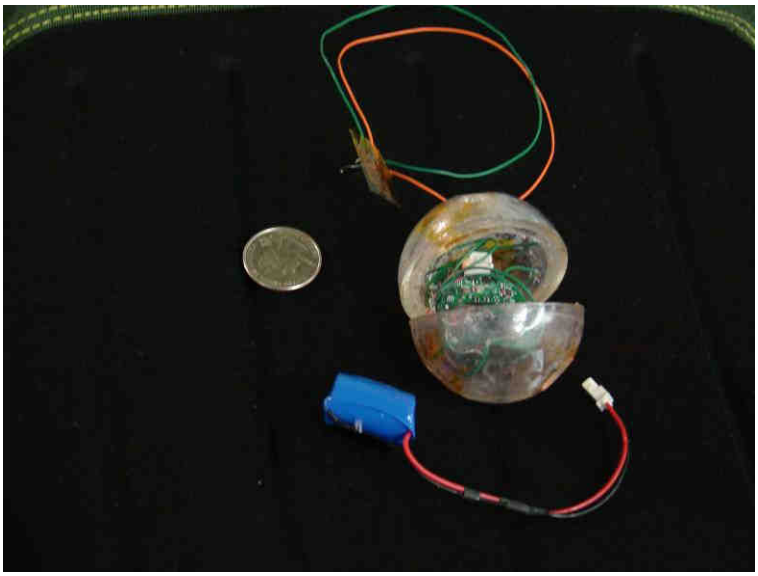

Figure 40: Photograph of one sensor used during flow loop trials.

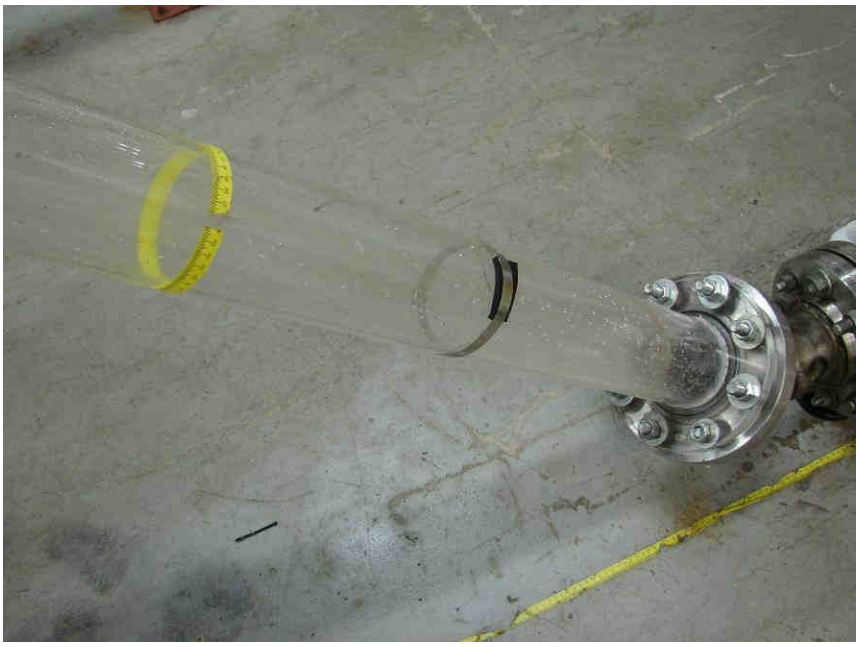

Figure 41: Photograph of water spray in flow loop test (note sensor is located at the bottom of the curve but is not visible).

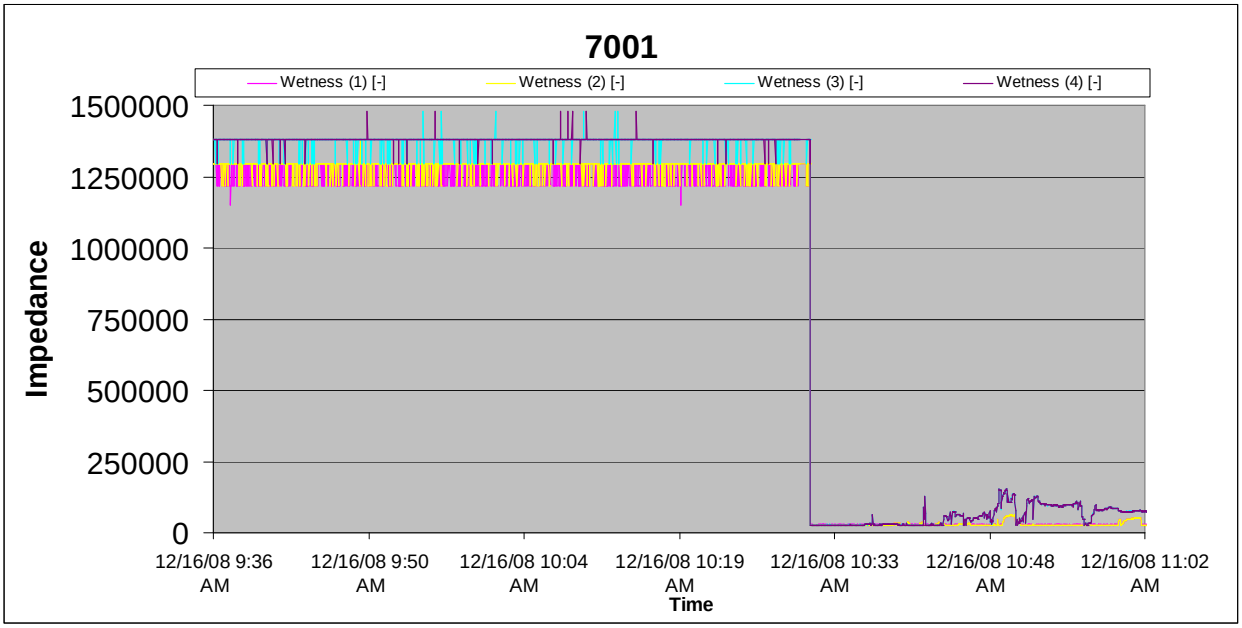

Figure 42: Results from first sensor ball during second round of testing.

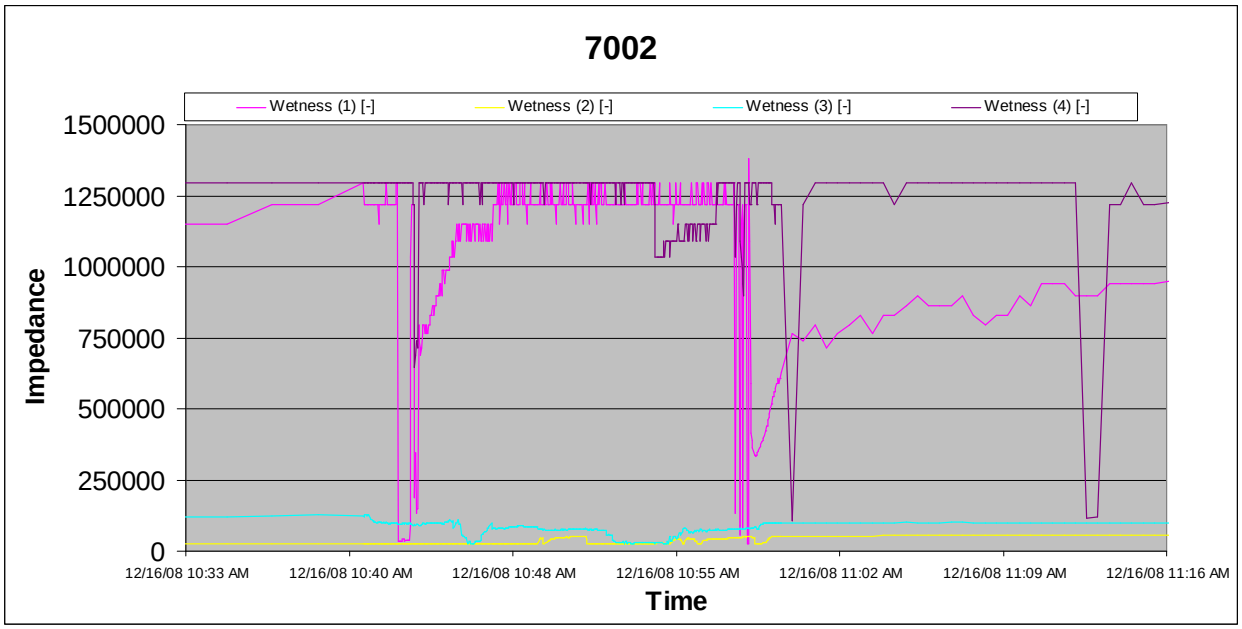

Figure 43: Results from second sensor ball during second round of testing.

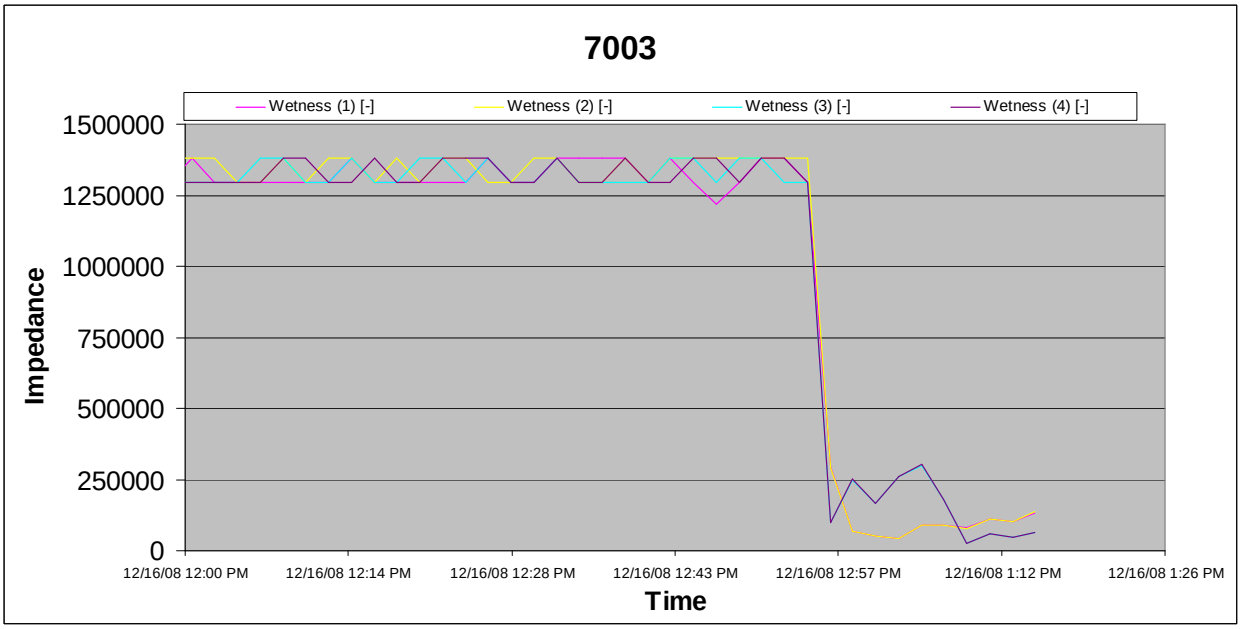

Figure 44: Results from third sensor ball during second round of testing.

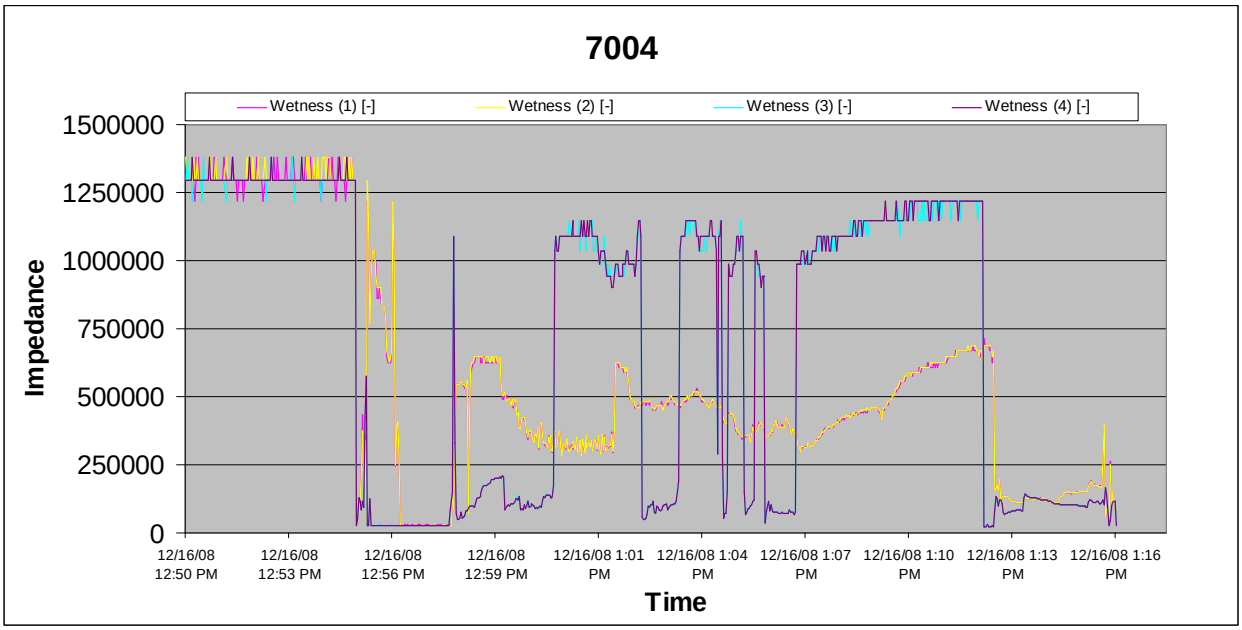

Figure 45: Results from forth sensor ball during second round of testing.

4 CONCLUSIONS AND TECHNOLOGY IMPLEMENTATION

Pipelines pose an enormous challenge to monitoring because of their geographic extent, buried nature, and the need to provide relatively uninterrupted service. Therefore, any monitoring/inspection technology that require excavation or significant interruption of operations are unlikely to be adopted easily. The developed technology aims to provide a monitoring tool that will be more easily adopted because it overcomes many of the limitations of existing technologies. In addition, this technology can be adapted to provide feedback control to various mitigation schemes such as inhibitor or biocide injections. The introduction of an instrumented sphere that can form an internal communication network and communicate the data to an outside receiver is a novel concept.

Through the course of this project, each of the component technologies and concepts have been successfully demonstrated. Several fully functional prototype systems have been constructed and evaluated thereby going a long way towards validating the technology. Even though much has been accomplished and the sensor systems have been successfully validated in the flow loop tests, some challenges still remain for full industry acceptance and adoption. Based on input from pipeline operators at the first and second flow loop validation trials, these issues need to be addressed:

- Install sensors on cleaning pig for first field trial – It was suggested that this be viewed as an intermediary step prior to injection of the sensor balls directly into the pipeline. Thus, the next set of field validation trials should involve installing the sensor systems onto a set of cleaning pigs. The reasoning being that the pigs

are already approved for use in pipeline systems and already have multiple components and systems on them so adding one more should be straight forward. Once a few successful runs with the sensors installed on pigs has been demonstrated, it would then be an easier step to then take them off the pigs and run them as independent sensor balls inside the pipeline. The suggested next steps are to:

- Contact cleaning pig companies and get design information
- Possible design for a sensor wheel on front of cleaning pig
- Sensor wheel mounted on back of dewatering pig – how good is the dewatering
- Acquire some cleaning pigs and conduct trial run(s)

o Improvement of sensor systems and packaging – As discussed previously, the epoxy adhesive used to attach the thin film corrosivity/water detection sensors to the balls appeared to be softened when exposed to mineral oils during the second round of flow loop validation trials. An alternative approach using printed circuit board sensor elements instead of thin films with a modified attaching scheme has already been devised and should be tested. Evaluation of this combined with the possible use of a polyurethane top coat to improve impact resistance should also be explored. The suggested next steps are to:

- Explore collaboration with standard probe manufacturers (e.g., Rohrback Cosasco, Roxar, Metal Samples, etc.) for sensor packaging and antenna insertion
- Develop a quality control test protocol to verify sensor functionality and desired performance prior to use
  - Perhaps perform test using rotating wheel in autoclave
  - Explore possible use of Battelle, SwRI, or U of Tulsa flow loops

It was suggested by the operating pipeline company personnel at the second flow loop validation trial that the scope of the pending follow on project for conducting field trials in dry gas pipelines be modified to address these two aspects. Furthermore, it was emphasized that the primary goal should be to approach the field validation trials in a two stage approach with the first stage aimed at installing the sensors on cleaning pigs and the second then to use the sensors as independent balls. The packaging modification and improvements and other issues would be explored in parallel with the pig installation trials.